normal children. Fetal chromosomes were analyzed by GTG banding and multi-color fluorescent in situ hybridization (mFISH) using cultured amniocytes. After cytogenetic analyses, she was informed that one chromosome 5 with interstitial deletion and a small marker ring chromosome were detected in all the cells. Then, chromosomal analysis of the parents was performed on peripheral blood and showed normal karyotyes. It was difficult to offer additional molecular analyses within a limited term for pregnancy interruption. Ultrasonographic examination at 19 weeks of gestation did not detect any specific abnormality in the fetus. Despite possible unfavorable prognosis informed in genetic counseling, she and her spouse decided against termination of the pregnancy.

The pregnancy was uneventful and she delivered a phenotypically normal boy at 39 weeks of gestation. Apgar score was 8/8 and there were no particular clinical features. Body length, weight, and head circumference were within the normal range: 48 cm, 2,916 g, and 33 cm, respectively. After birth, we received informed consent to examine aCGH and BAC-FISH for further confirmation of the diagnosis.

Developmental, physical, and neurological examinations were normal and he appropriately reached his milestones. At 1 year and 6 months, his developmental quotient (DQ) was 110 (Fig. 1); echocardiography and brain imaging were also normal.

MOLECULAR CYTOGENETICSTUDIES

Chromosome and FISH Analyses

Cultured amniocytes were analyzed using G-banding with 540 bands per haploid number. G-banded chromosomes demonstrated

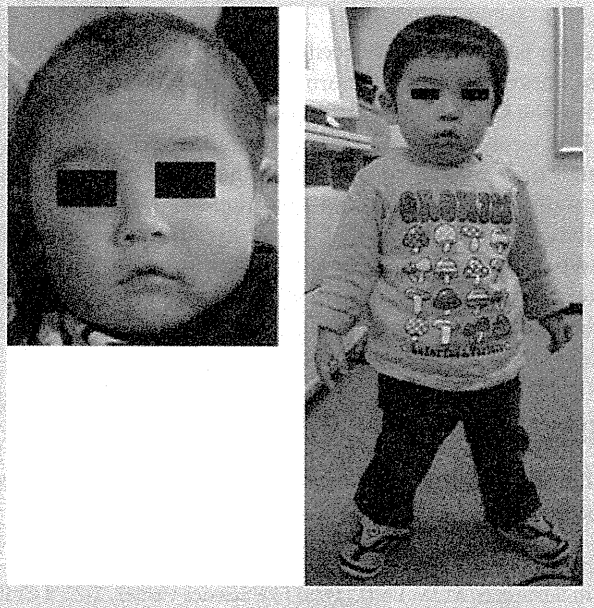

FIG. 1. Propositus at age 8 months (left picture) and 1 year 6 months (right picture). Note the phenotypically normal boy.

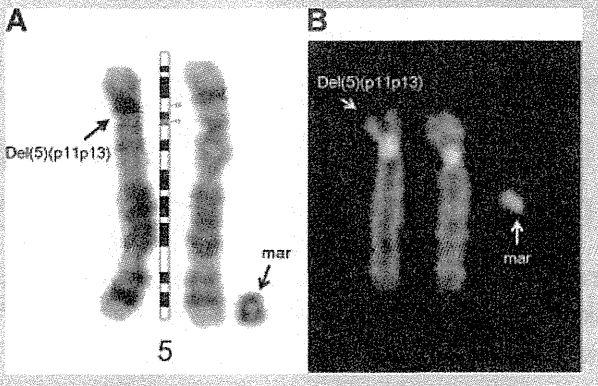

FIG. 2. Partial karyogram of chromosome 5, del(5p), and supernumerary ring by G-banding (A) and mFISH (B).

that all cells had an interstitial deletion of chromosome 5 (5p11 → p13), and a small marker ring chromosome (Fig. 2A). The origin of this marker chromosome was unclear by G-banding. Therefore, the initial karyotyping was 47,XY,del(5)(p11p13), +mar. The mFISH revealed that the marker ring originated from chromosome 5, the same as the deleted chromosome (Fig. 2B). The ring chromosome seemed to have a centromere because this marker was detected in all cells. Chromosome analysis of the parents showed no abnormalities, indicating that these structural abnormalities in the fetus were de novo.

Oligonucelotide aCGH

For detection of gain and loss of chromosome segments, oligonucleotide-based microarray analysis was performed on reserved cultured amniocytes using a 105K-feature whole-genome microarray (Signature Chip Oligo Solution®, made for Signature Genomic Laboratories by Aligent Technologies Inc., Santa Clara, CA) [Ballif et al., 2008]. Microarray analysis of 1543 loci using on oligonucleotide array detected a complex abnormality in the DNA obtained from cultured amniocytes. Based on microarray analysis, this fetus had two duplications and a deletion of the short arm of chromosome 5. This abnormality was first characterized by a single copy gain of 380 oligonucleotide probes from the terminal end of the short arm of 5p, at 5p15.33p15.31. The extent of this duplication has been estimated to be approximately 6.1 Mb. The second alteration was characterized by a single copy loss of 347 oligonucleotide probes from 5p14.3p13.2. The extent of this interstitial deletion is estimated to be approximately 15.3 Mb. The third alteration was characterized by a single copy gain of 147 oligonucleotide probes from the pericentric region at 5p12p11. The extent of this duplication has been estimated to be approximately 3.4 Mb. Thus, this complex alteration resulted in partial trisomy 5p15.33–p15.31, partial monosomy 5p14.3–p13.2, and partial trisomy 5p12–p11. In conclusion, the result of microarray was arr5p15.33–p15.31(131,945–6,267,160)x3, 5p14.3–p13.2(21,438,495–36,736,934)x1, 5p12–p11(42,529,343–45,908,725)x3 (Fig. 3).

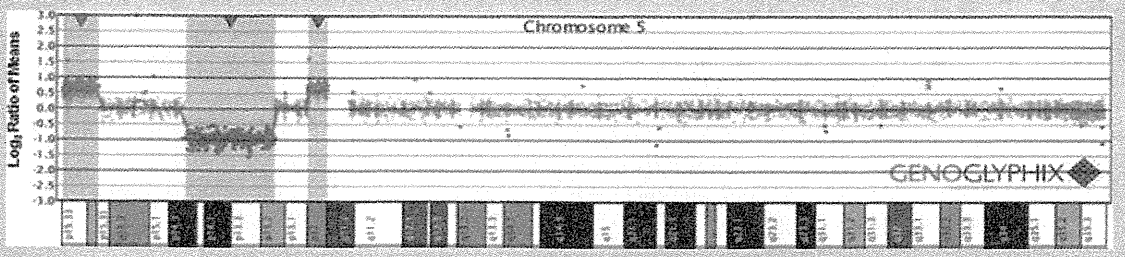

FIG. 3. Microarray plot showing, from left to right, a single copy gain of 380 oligonucleotide probes at 5p15.33p15.31, approximately 6.1 Mb in size; a single copy loss of 347 oligonucleotide probes from 5p14.3p13.2, approximately 15.3 Mb; and single copy gain of 147 oligonucleotide probes at 5p12p11, approximately 3.4 Mb in size. Probes are ordered on the x-axis according to physical mapping positions, with the distal p-arm on the left and the distal q-arm on the right.

BAC-FISH

For confirmation of the array results, FISH analyses were performed with BAC clones from duplicated and deleted regions as previously described [Shaffer et al., 1994; Traylor et al., 2009]. For this study, we used cord blood obtained at delivery.

FISH using a BAC clone from the 5p14.2 deleted region (RP11-701M20) and the 5p15.33 duplicated region (RP11-1006P13) identified an abnormal deleted (del) chromosome 5 that showed the loss of hybridization signals from the deleted region at 5p14.2 (Fig. 4A) and the presence of hybridization signals from the duplicated region at 5p15.33 (Fig. 4C). Interphase FISH

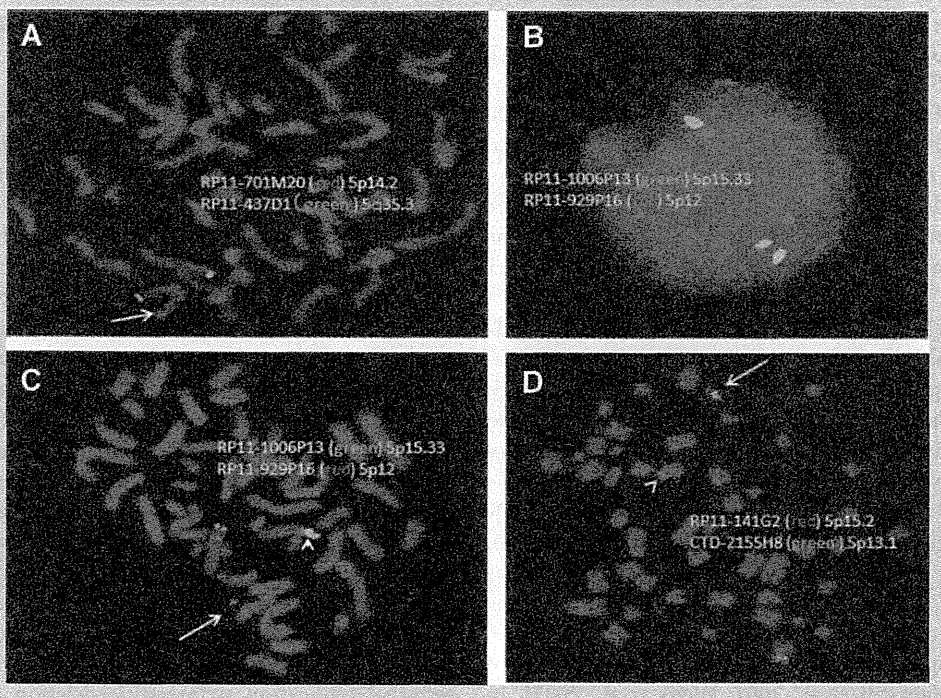

FIG. 4. FISH characterizations of a complex rearrangement on the short arm of chromosome 5. A: FISH showing a deletion of 5p14.2, BAC clone RP11-701M20 from 5p14.2 is labeled in red, and RP11-437D1 from 5q35.3 is labeled in green as a control. The presence of one red signal indicates deletion of 5p14.2 on one homologue (arrow). B,C: FISH with probes from the two regions is shown to be present in three copies by aCGH. BAC clone RP11-1006P13 from 5p15.33 is labeled in green, and RP11-929P16 from 5p12 is labeled in red. Interphase FISH (B) confirmed the presence of three copies of both regions. Metaphase FISH (C) shows a red signal but not a green signal on a small, supernumerary ring chromosome (arrow), indicating the presence of the 5p12 material on the supernumerary chromosome. Dotted green signals from 5p15.33 were present on the normal chromosome 5 homologs, but terminal duplicated signals were observed on one chromosome 5 (arrow head). D: FISH with probes from the intervening regions shown to be present in two copies by aCGH. BAC clone RP11-141G2 from 5p15.2 is labeled in red, and CTD-2155H8 from 5p13.1 is labeled in green. The supernumerary ring chromosome (arrow) shows a green signal and therefore the presence of material from 5p13.1, while one chromosome 5 homolog (arrowhead) shows a deletion for this region. The probe from 5p15.2 shows a normal hybridization pattern.

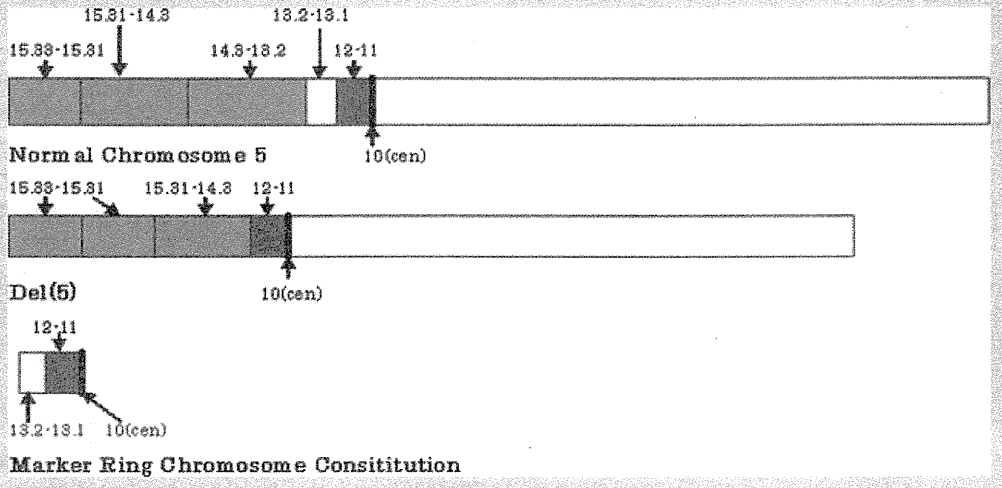

FIG. 5. Molecular background information on the deleted chromosome 5 and marker ring chromosome.

(Fig. 4B) clarified the presence of three copies of 5p15.33 and 5p12 regions. This del(5) also showed hybridization signals in an experiment using BAC clones from the first normal intervening sequence, between the terminal duplication and the deleted region, at 5p15.2 (RP11-141G2; Fig. 4D). Additional FISH analysis using a BAC clone from the 5p12 duplicated region (RP11-929P16) confirmed the origin of the marker ring chromosome (Fig. 4C). Hybridization signals from the second intervening normal sequence at 5p13.1 (CTD-2155H8), between the deleted region and the pericentric duplicated region, were also present on the marker ring chromosome, but not on the del(5), indicating that the deletion on that chromosome extends from 5p14.3 through 5p13.1 (Fig. 4D).

In conclusion, this baby had two abnormal derivative chromosomes. The first der(5) had an abnormal short arm with a duplication of 5p15.31 → 5p15.33, and a deletion of 5p13.1 → p14.3. The second der(5), the marker ring chromosome, was comprised of material from 5p10 → p13.2 (Fig. 5). The final karyotype of the baby is: 47,XY,ish der(5)(pter → p15.31::pter → p14.3::p11 → qter)(RP11-1006P13++,RP11-141G2+,RP11-701M20−,CTD-2155H8−),+der(5)(:13.2 → p10:)(CTD-2155H8+,RP11-929P16+).

DISCUSSION

Partial deletion of 5p is often seen in prenatal diagnoses and newborn analyses [Mainardi et al., 2001; Weiss et al., 2003]. In autosomes other than chromosome 5, deletions involving various chromosomes have also been reported in the literature [Gardner and Sutherland, 1996; Ryan et al., 1997; Slavotinek and Kingston, 1997]. Partial deletion of autosomes is generally accompanied by mild-to-severe clinical symptoms, including mental and developmental retardation in babies, although there have been exceptional cases where no clinical symptoms are observed [Callen et al., 1993; Overhauser et al., 1994; Knight et al., 1995]. Supernumerary marker chromosomes including small rings are also seen frequently in prenatal diagnoses [Michalski et al., 1993; Brøndum-Nielsen and Mikkelsen, 1995; Karaman et al., 2006]. Among babies with such small markers, some cases have no clinical features, but others showed mild-to-severe abnormalities after birth [Callen et al., 1993; Overhauser et al., 1994; Knight et al., 1995; Gardner and Sutherland, 1996; Daniel and Malafiej, 2003; Liehr et al., 2004; Bernardini et al., 2007]. Thus, in genetic counseling, it is important to offer chromosomal information from prenatal diagnoses and to provide as much detail as possible, including the origin and inheritance.

The present case had a deletion and a supernumerary marker ring chromosome. To our knowledge, this is the first report of detection by prenatal screening of both a deletion and a marker ring. In the literature, there are some mosaic cases of clones with a deletion and an additional ring separately [Gutiérrez-Angulo et al., 2002; Gereltzul et al., 2008; Kara et al., 2008], but such cases are extremely rare. In newborn infants, only one other case has been reported [Schuffenhauer et al., 1996] with a deletion and a ring of chromosome 5; this baby showed a mosaicism of 46,XY,del(5)/47,XY, del(5),+dic(5), with macrocephaly, asymmetric square skull, minor facial anomalies, omphalocele, inguinal hernias, hypospadias, and club feet. The break points of the deletion shared cen and p13 with those of the dicentric ring chromosome; this case had partial duplication of 5p (p13 → cen), and the mechanisms of del(5) and dic(5) were relatively straightforward. In the present case, on the other hand, the mechanisms of del(5) and marker ring [r(5)] were extremely complex. Microarray analysis revealed a terminal duplication, an interstitial deletion, and a pericentromeric duplication of the short arm of chromosome 5. Through this analysis, a total of six break points of the short arm of chromosome 5 (p15.33, p15.31, p14.3, p13.2, p12, and p11) were related to the formation of the structural abnormality with the duplication and the deletion, and the marker ring. According to the results of the G-band analysis of this case, we determined the break points of del(5) to be p11 and p13. However, assuming the microarray data are correct, the composition of r(5) becomes complicated, and explanation of the underlying mechanisms becomes difficult. To facilitate understanding of the exact composition of del(5) and r(5),

we performed FISH analysis using BAC clones from the duplicated 5p15.33, 5p12 regions and deleted 5p14.2 region. The short arm of the del(5) revealed a duplication of 5p15.31 → 5p15.33 and a deletion of 5p13.1 → p14.3. The r(5) was comprised of material from 5p10 → p13.2. Although supernumerary ring chromosome formation is difficult to determine, we speculate that this case have resulted from "centromere misdivision" along with a break in either the p or q arm, forming a small ring chromosome [Baldwin et al., 2008].

In summary, this complex 5p abnormality was characterized by a terminal duplication of 5p15.33p15.31 of approximately 6.4 Mb, an interstitial deletion 15p14.3p13.2 of approximately 15.3 Mb and an interstitial duplication of 5p12p11 of approximately 3.4 Mb. The 5p terminal duplication contained at least 21 genes including ADAMTS16, AHRR, and C5orf38. The 5p14.3p13.2 deletion lacked at least 22 genes including *CDH12*, *PRDM9*, *CDH10*, and *DH9*. The 5p12p11 duplication contained at least 11 genes including *GHR*, *SEPP1*, *C5orf39*, and *ZNF11131*.

When the child was examined at 1 year and 6 months, we could not find any developmental abnormality, either physical or mental. Because of his age he will need to be followed to confirm normal intellectual development. In order to provide accurate and useful genetic counseling in similar cases in the future, the accumulation of further reports with complicated chromosome abnormalities would be beneficial.

REFERENCES

Baldwin EL, May LE, Justice AN, Martin CL, Ledbetter DH. 2008. Mechanism and consequences of small supernumerary marker chromosomes: From Barbara McClintock to modern genetic-counseling issue. Am J Hum Genet 82:398–410.

Ballif BC, Theisen A, McDonald-McGinn DM, Zackai EH, Bejjanni BA, Shaffer LG. 2008. Identification of a previously unrecognized microdeletion syndrome of 16q11.2q12.2. Clin Genet 74:469–475.

Bernardini L, Capalbo A, D'Avanzo MG, Torrente I, Grammatico P, Dell'Edera D, Cavalcanti DP, Novelli A, Dallapiccola B. 2007. Five cases of supernumerary small ring chromosomes 1: Heterogeneity and genotype–phenotype correlation. Eur J Med Genet 50:94–102.

Brøndum-Nielsen K, Mikkelsen M. 1995. A 10-year survey, 1980–1990, of prenatally diagnosed small supernumerary marker chromosomes, identified by FISH analysis. Outcome and follow-up of 14 cases diagnosed in a series of 12,699 prenatal samples. Prenat Diagn 15:615–619.

Callen DF, Eyre H, Lane S, Shen Y, Hansmann I, Spinner N, Zackai E, McDonald-McGinn D, Schuffenhauer S, Wauters J, Van Thienen M-N, Van Roy B, Sutherland GR, Haan EA. 1993. High resolution mapping of interstitial long arm deletions of chromosome 16: Relationship to phenotype. J Med Genet 30:828–832.

Daniel A, Malafiej P. 2003. A series of supernumerary small ring marker autosomes identified by FISH with chromosome probe arrays and literature review excluding chromosome 15. Am J Med Genet Part A 117A:212–222.

Gardner RJM, Sutherland GR. 1996. Chromosome Abnormalities and Genetic Counseling. 2nd edition. New York, Oxford: Oxford University Press. pp. 1–478.

Gereltzul E, Baba Y, Suda N, Shiga M, Inoue MS, Tsuji M, Shin I, Hirata Y, Ohyama K, Moriyama K. 2008. Case report of de novo dup(18p)/del-(18q) and r(18) mosaicism. J Hum Genet 53:941–946.

Gutiérrez-Angulo M, Lazalde B, Vasquez AI, Leal C, Corral E, Rivera H. 2002. del(X)(p22.1)/r(X)(p22.1q28) Dynamic mosaicism in a Turner syndrome patient. Ann Genet 45:17–20.

Kara N, Okten G, Guns SO, Saglam Y, Tasdemir HA, Pinarli FA. 2008. An epileptic case with mosaic ring chromosome 6 and 6q terminal deletion. Epilepsy Res 80:219–223.

Karaman B, Aytan M, Yilmaz K, Toksoy G, Onal EP, Ghanbari A, Engur A, Kayserili H, Yuksel-Apak M, Basaran S. 2006. The identification of small supernumerary marker chromosomes; the experiences of 15,792 fetal karyotyping from Turkey. Eur J Med Genet 49:207–214.

Knight LA, Yong MH, Tan M, Ng IS. 1995. Del(3) (p25.3) without phenotypic effect. J Med Genet 32:994–995.

Liehr T, Claussen U, Starke H. 2004. Small supernumerary marker chromosomes (sSMC) in humans. Cytogenet Genome Res 107:55–67.

Mainardi PC, Perfumo C, Calì A, Coucourde G, Pastore G, Cavani S, Zara F, Overhauser J, Pierluigi M, Bricarelli FD. 2001. Clinical and molecular characterization of 80 patients with 5p deletion: Genotype–phenotype correlation. J Med Genet 38:151–158.

Michalski K, Rauer M, Williamson N, Perszyk A, Hoo JJ. 1993. Identification, counselling, and outcome of two cases of prenatally diagnosed supernumerary small ring chromosomes. Am J Med Genet 46:88–94.

Overhauser J, Huang X, Gersh M, Wilson W, McMahon J, Bengtsson U, Rojas K, Meyer M, Wasmuth JJ. 1994. Molecular and phenotypic mapping of the short arm of chromosome 5: Sublocalization of the critical region for the cri-du-chat syndrome. Hum Mol Genet 3:247–252.

Ryan AK, Goodship JA, Wilson DI, Philip N, Levy A, Seidel H, Schuffenhauer S, Oechsler H, Belohradsky B, Prieur M, Aurias A, Raymond FL, Clayton-Smith J, Hatchwell E, McKeown C, Beemer FA, Dallapiccola B, Novelli G, Hurst JA, Ignatius J, Green AJ, Winter RM, Brueton L, Brøndum-Nielsen K, Stewart F, Van Essen T, Patton M, Paterson J, Scambler PJ. 1997. Spectrum of clinical features associated with interstitial chromosome 22q11 deletions: A European collaborative study. J Med Genet 34:798–804.

Schuffenhauer S, Kobelt A, Daumer-Haas C, Löffler C, Müller G, Murken J, Meitinger T. 1996. Interstitial deletion 5p accompanied by dicentric ring formation of the deleted segment resulting in trisomy 5p13-cen. Am J Med Genet 65:56–59.

Shaffer LG, McCaskill C, Han J-Y, Choo KHA, Cutillo DM, Donnenfeld AE, Weiss L, Van Dyke DL. 1994. Molecular characterization of de novo secondary trisomy 13. Am J Hum Genet 55:968–974.

Slavotinek A, Kingston H. 1997. Interstitial deletion of bands 4q12 → q13.1: Case report and review of proximal 4q deletions. J Med Genet 34:862–865.

Traylor R, Fan Z, Ballif BC. 2009. Micordeletion of 6q16.1 encompassing EPHA7 in a child with mild neurological abnormalities and dysmorphic features: Case report. Mol Cytogenet 2:1–6.

Weiss A, Shalev S, Weiner E, Shneor Y, Shalev E. 2003. Prenatal diagnosis of 5p deletion syndrome following abnormally low maternal serum human chorionic gonadotrophin. Prenat Diagn 23:572–574.

ELSEVIER

Brain & Development 33 (2011) 576–579

BRAIN & DEVELOPMENT
Official Journal of the Japanese Society of Child Neurology

www.elsevier.com/locate/braindev

Original article

A familial case of LEOPARD syndrome associated with a high-functioning autism spectrum disorder

Yoriko Watanabe [a,1,*], Shoji Yano [b], Tetsuya Niihori [c], Yoko Aoki [c], Yoichi Matsubara [c], Makoto Yoshino [a], Toyojiro Matsuishi [a,1]

[a] *Department of Pediatrics and Child Health, Kurume University School of Medicine, 67 Asahi-machi, Kurume, Japan*
[b] *Genetics Division, Department of Pediatrics, LAC+USC Medical Center, Keck School of Medicine, University of Southern California, Los Angeles, CA, USA*
[c] *Department of Medical Genetics, Tohoku University School of Medicine, Sendai, Japan*

Received 6 July 2010; received in revised form 3 October 2010; accepted 6 October 2010

Abstract

A connection between LEOPARD syndrome (a rare autosomal dominant disorder) and autism spectrum disorders (ASDs) may exist. Of four related individuals (father and three sons) with LEOPARD syndrome, all patients exhibited clinical symptoms consistent with ASDs. Findings included aggressive behavior and impairment of social interaction, communication, and range of interests. The coexistence of LEOPARD syndrome and ASDs in the related individuals may be an incidental familial event or indicative that ASDs is associated with LEOPARD syndrome. There have been no other independent reports of the association of LEOPARD syndrome and ASDs. Molecular and biochemical mechanisms that may suggest a connection between LEOPARD syndrome and ASDs are discussed.

Keywords: LEOPARD syndrome, Noonan syndrome; Autism spectrum disorders (ASDs); RAS/MAPK signal transduction pathway

1. Introduction

LEOPARD syndrome (OMIM#151100) is a rare autosomal dominant disorder characterized by Lentigines, Electrocardiogram abnormalities, Ocular hypertelorism, Pulmonic valvular stenosis, Abnormalities of genitalia, Retardation of growth, and Deafness. This syndrome is caused by germline missense mutations in the *PTPN11* gene that encodes Src homology 2 domain-containing tyrosine phosphatase 2 (Shp2): non-receptor protein-tyrosine phosphatase comprising two N-terminal SH2 domains, a catalytic domain, and a C terminus with tyrosylphosphorylation sites and a proline-rich stretch. The mutations induce catalytically impaired Shp2 by a "dominant negative effect" [1–2].

In the more common Noonan syndrome, approximately 50% of patients have *PTPN11* mutations scattered over the entire Shp2, including the catalytic domain. The mutations resulting in the Noonan phenotype are the "gain-of-function" mutations, and they exhibit substantially increased catalytic ability. Although LEOPARD syndrome and Noonan syndrome are caused by *PTPN11* mutations resulting in opposite effects, they share many common clinical features, including physical dysmorphic findings and intellectual disability [1].

The term "autism spectrum disorders (ASDs)" was first used by Lorna Wing [3] and then widely used as a category comprised of autistic disorder, Asperger's

* Corresponding author. Tel.: +81 942 35 3311x3656; fax: +81 942 38 1792.
E-mail address: york@med.kurume-u.ac.jp (Y. Watanabe).
[1] The author contributed equally to this work.

0387-7604/$ - see front matter © 2010 The Japanese Society of Child Neurology. Published by Elsevier B.V. All rights reserved.
doi:10.1016/j.braindev.2010.10.006

disorder, and other related conditions [4]. These conditions are very common neurobehavioral disorders that are characterized by impairments in three behavioral domains, including social interaction, language/communication/imaginative play, and a range of interests and activities [3–5].

At least ten genes have been reported to be associated with ASDs [6]. Except for Rett syndrome, the other pervasive developmental disorder (PDD) subtypes including autistic disorder, Asperger's disorder, disintegrative disorder, and PDD Not Otherwise Specified (PDDNOS) are not tightly linked to any particular gene mutations. Several common genetic syndromes are known to be associated with ASDs. Autism is frequent in patients with tuberous sclerosis (TSC) [7], with neurofibromatosis type 1 [8,9] and with Fragile X syndrome [10]. Studies of psychological profiles of adults with Noonan syndrome did not suggest a specific behavioral phenotype, but difficulties with social competence and emotional perceptions were noted [11]. A case of Noonan syndrome who was also diagnosed with autism was reported [12]. The present study of neuropsychiatric evaluation in a familial case of LEOPARD syndrome indicates all patients satisfied the criteria of ASDs. An association of LEOPARD syndrome and ASDs has not been reported previously. The familial case presented in this report may suggest such an association.

2. Patients and methods

After obtaining written informed consent, fifteen coding exons in *PTPN11* were sequenced in each patient following the methods described somewhere else [13].

Diagnostic and Statistical Manual of Mental Disorders, Fourth Edition (DSM-IV-TR) [5] and The high-functioning Autism Spectrum Screening Questionnaire (ASSQ) [14] were used in neuropsychiatric evaluation of the subjects.

Patient 1 is a 20-year-old male who was born as the second child to a non-consanguineous Japanese couple. His early developmental milestones were reportedly unremarkable. He was clinically diagnosed with LEOPARD syndrome at age 7 years based on findings that included lentigines, multiple café-au-lait spots, electrocardiogram (ECG) abnormalities, ventricular septal defect, ocular hypertelorism, short stature, and unilateral renal hypoplasia. *PTPN11* mutation analysis revealed a heterozygous mutation of 1403C > T (T468 M). The patient was diagnosed as having Asperger's disorder based on ASSQ and DSM-IV-TR, at age 12 years. His intelligence quotient (IQ) by the Wechsler Intelligence Scale for Children-third edition (WISC-III) was 85 (verbal: 77, performance 98). His ASSQ score by mother's rating was 41. He met the DSM-IV-TR diagnostic criteria of Asperger's disorder with all subcategories in the category of Qualitative impairment in social interaction (Category 1), three subcategories (1,2, and 4) in the category of Restricted repetitive and stereotyped patterns of behavior, interests and activities (Category 2), and the rest of the four categories (Table 1).

Patient 2 is a 15-year-old younger brother of Patient 1. His early infantile developmental milestones were unremarkable. He was diagnosed with growth retardation at age 2½ years. At age 12 years his clinical findings of a few café-au-lait spots, ocular hypertelorism, and undescended testes led us to obtain *PTPN11* mutation analysis, which showed the same heterozygous mutation of 1403C > T. At age 9 years, a diagnosis of Asperger's disorder was made based on ASSQ and DSM-IV-TR. His full-scale IQ by WISC-III at age 9 years was 99 (verbal 104, performance 92). His ASSQ score by parental rating was 32 at age 15 years. He also met the Asperger's disorder diagnostic criteria with all subcategories of Category 1, three of Category 2 (1, 2, and 4), and the rest of the categories (Table 1).

Patient 3 is the 22-year-old eldest brother of Patients 1 and 2. His developmental milestones were normal, although his ritualistic behavior and difficulties in relating to peers were noted in his childhood. He had a surgical repair of bilateral undescended testes and inguinal hernia. He was diagnosed with Wolff-Parkinson-White syndrome at age nine years. He has ocular hypertelorism and short stature. The same *PTPN11* heterozygous mutation found in the two younger siblings was identified in this patient. He attends college, and was diagnosed as having PDDNOS, because he also had impaired development of reciprocal social interaction associated with communication skills, repetitive routine, and ritualistic behavior. His ASSQ score was 7 at age 22 years (Table 1).

Patient 4 is a 55-year-old male who is the father of the siblings. He has prominent lentigines, bilateral mild hearing loss, cardiac anomalies, ECG abnormalities, short stature, and apparent ocular hypertelorism. His early developmental milestones are not well known. He has been noted to have obsession with a specific topic, repetitive routine and rituals, and clumsy movements. At age 50 years, his social skills and aggressive behavior were noted to be deteriorating, and consequently he was suspected of having Asperger's disorder based on DSM-IV-TR. He met the diagnostic criteria of Asperger's disorder with Category 1 (1 and 3), Category 2 (1 and 2), and the rest of the four categories. His ASSQ score was 20 at age 55 years by his wife's evaluation. He has the same heterozygous *PTPN11* mutation (Table 1).

3. Discussion

The presented familial case of LEOPARD syndrome included individuals (patients 1, 2, and 4) diagnosed with or suspected of having Asperger's disorder, and

Table 1
Summary of clinical findings and *PTPN11* mutation.

	Pt. 1 Male	Pt. 2 Male	Pt. 3 Male	Pt. 4Male
Age	20 y	15 y	22 y	55 y
Physical findings				
Skin: café-au-lait spots	multiple	a few	a few	a few
Lentigines	+++	+++	-	+++
Cardiac defects	VSD	No	No	No
EKG abnormalities	+	No	WPW	No
Ocular hypertelorism	+	+	+	+
Pulmonary stenosis	No	No	No	No
Abnormal genitalia	No	Und. Testes*	Und. Testes*	No
Renal anomalies	R-hypoplasia	No	No	No
Retardation of growth	Yes	+	+	No
Deafness	No	No	No	Yes
Miscellaneous:				
Rocker bottom feet	Yes	Yes	Yes	No
Macrocephaly	Yes	Yes	Yes	No
PTPN11 mutation	T468 M	T468 M	T468 M	T468 M
Neuropsychological				
Diagnosis	AD**	AD**	PDDNOS***	AD**
ASSQ score[1] (age)	41 (12 y)	32 (15 y)	7 (22 y)	20 (50 y)
WISC-III[2] (age)	85 (12 y)	99 (9 y)	n/a	n/a
-Verbal/performance	77/98	104/92	n/a	n/a

* Und. Testes, undescended testes.
** AD, Asperger's disorder.
*** PDDNOS, Pervasive developmental disorder not otherwise specified.
[1] ASSQ score, Autism Spectrum Screening Questionnaire Score. The cutoff score of 3 predicts 91% of the true positive rate of Autistic spectrum disorders.
[2] WISC-III, Wechsler Intelligence Scale for Children-third edition.

patient 3 was diagnosed as having PDDNOS, which may lead to the diagnosis of ASD. ASDs were first introduced by Lorna Wing, who suggested that Asperger's disorder is a type of ASD and described in detail its various manifestations in speech, nonverbal communication, social interaction, motor coordination, motor clumsiness, and idiosyncratic interests [3]. Patient 3 did not have enough clinical symptoms to meet the diagnostic criteria for Asperger's disorder; however, he had some symptoms suggestive of ASD in his childhood that led to a diagnosis of PDDNOS.

The ASSQ is a 27-item checklist for completion by lay informants when assessing characteristic symptoms of Asperger's disorder and high-functioning autism in children and adolescents with normal intelligence or mild mental retardation. The ASSQ allows for rating on a 3-point scale (0, 1, or 2; 0 indicating normality, 1 some abnormality, and 2 definite abnormality). The range of possible scores is 0–54. The mean ASSQ parent scores in the Asperger's disorder validation sample were 25.1 (SD, 7.3) [14]. The cutoff score of 13 is 91% of the true positive rate of ASDs. The ASSQ score was established as a screening tool primarily for children between 6 and 17 years of age by parents and/or teachers. The delayed evaluation of patient 3 may account for the difference in diagnosis between this patient and his siblings.

ASDs are known to be associated with particular genetic disorders such as fragile X syndrome [10,15,16], tuberous sclerosis (TSC) [7], and neurofibromatosis type 1 [8,9]. Fifty percent of children with TSC have behavioral problems in the form of ASDs. Gene mutations in either *TSC1* or *TSC2* influence neural precursors, resulting in abnormal cell differentiation and dysregulated control of cell size. These cells migrate to the cortex to generate an abnormal collection of inappropriately positioned neurons, causing widespread cortical disorganization and structural abnormalities [7]. Mutations in *PTPN11* causing LEOPARD syndrome induce catalytically impaired Shp2. In situ hybridization detected Shp2 expression in the neural ectoderm and nervous system in mouse embryos, suggesting an involvement of Shp2 in neural development. Shp2 is a critical signaling molecule in the coordinated regulation of progenitor cell proliferation and neuronal/astroglial cell differentiation. The studies with mutant mouse strains with Shp2 selectively deleted in neural precursor cells showed a dramatic phenotype of growth retardation, early postnatal lethality, and multiple defects in proliferation and cell fate specification in neural stem/progenitor cells [17]. The product of the TSC2 gene tuberin is known to up-regulate the B-RAF/MEK/MAPK signal transduction pathway. B-RAF is required for neuronal differentiation, suggesting another possible link between B-RAF signaling and the clinical manifestations of TSC including ASDs [18]. Disturbed neuronal cell differentiation and development due to mutations in

the TSC genes and the *PTPN11* gene are likely to contribute to the development of ASDs in patients with these syndromes.

NF-I is well known to be associated with ASDs. The prevalence of autism in patients with NF-I was reported to be 4% [9]. The well-known function of the NF-I protein is to act as a RAS-GTPase-activating protein known to be involved in the regulation of the RAS-mitogen-activated protein kinase (MAPK) pathway. Mutations in the NF-I gene are thought to result in activation of the RAS/MAPK signal transduction pathway [2]. Clinical overlap between LEOPARD syndrome and NF-I is also well known [19].

Approximately 50% of patients with Noonan syndrome are due to missense *PTPN11* mutations [20]. *PTPN11* encodes SHP2, a protein tyrosine phosphatase, that is involved in the activation of the RAS/MAPK cascade [2]. Noonan syndrome is caused by "gain of function" *PTPN11* mutations [1,2], and the SHP2 mutants due to the *PTPN11* mutations causing Noonan syndrome cause prolonged activation of the RAS/MAPK pathway [2]. Schubbert et al. [21] reported that germline KRAS mutations cause Noonan syndrome through the hyperactive RAS/MAPK pathway.

Herault et al. [22] reported a positive association of the HRAS gene and autism. The psychological profiles of adults and children with Noonan syndrome have been studied, and deficiencies in social and emotional recognition and expression have been identified in adults, while low verbal IQ, clumsiness, and impairment of developmental coordination have been reported in children [23].

To date, there have been no reports to suggest an association of LEOPARD syndrome and ASDs. Our observations in this familial case may suggest at least some degree of association between LEOPARD syndrome and ASD phenotypes possibly through the RAS/MAPK signal transduction pathway. Further studies with more patients with LEOPARD syndrome are needed to establish the association and to investigate the genetic contributing factors causing ASDs, leading to the prevention and earlier detection of ASDs and better management of patients with these disorders.

References

[1] Kontaridis M, Swanson KD, David FS, Barford D, Neel BG. PTPN11 (Shp2) mutations in LEOPARD syndrome have dominant negative, not activating, effects. J Biol Chem 2006;281:6785-92.

[2] Aoki Y, Niihori T, Narumi Y, Kure S, Matsubara Y. The RAS/MAPK syndromes:novel roles of the RAS pathway in human genetic disorders. Hum Mutat 2008;29:992-1006.

[3] Wing L. Autistic spectrum disorders. BMJ 1996;312:327-8.

[4] Khouzam HR, El-Gabalawi F, Pirwani N, Priest F. Asperger's disorder: a review of its diagnosis and treatment. Comp Psychiatr 2004;45:181-91.

[5] American Psychiatric Association. Diagnostic and Statistical Manual of Mental Disorders. 4th ed.-Text Revision. Washington, DC: American Psychiatric Association; 2000.

[6] Muhle R, Trentacose SV, Rapin I. The genetics of autism. Pediatrics 2004;113:e472-86.

[7] Curatolo P. Tuberous sclerosis: genes, brain, and behavior. Dev Med Child Neurol 2006;48:404.

[8] Gillberg C, Forsell C. Childhood psychosis and neurofibromatosis-More than a coincidence? J Autism Dev Disord 1984;14:1-8.

[9] Williams PG, Hersh JH. The association of neurofibromatosis Type 1 and autism. J Autism Dev Disord 1998;28:567-71.

[10] Cohen IL, Sudhalter V, Pfadt A, Jenkins EC, Brown WT, Vietze PM. Why are autism and the fragile-X syndrome associated? Conceptual and methodological issues. Am J Hum Genet 1991;48:195-202.

[11] Verhoeven W, Wingbermuhle E, Egger J, Van der Burgt I, Tuinier S. Noonan syndrome: psychological and psychiatric aspects. Am J Med Genet A 2008;146A:191-6.

[12] Ghaziuddin M, Bolyard B, Alessi N. Autistic disorder in Noonan syndrome. J Intell Disabil Res 1994;38:67-72.

[13] Niihori T, Aoki Y, Ohashi H, Kurosawa K, Kondoh T, Ishikiriyama S, et al. Functional analysis of PTPN11/SHP-2 mutants identified in Noonan syndrome and childhood leukemia. J Hum Genet 2005;50:192-202.

[14] Ehlers S, Gillberg C, Wing L. A screening questionnaire for Asperger syndrome and other high-functioning autism spectrum disorders in school age children. J Autism Dev Disord 1999;29:129-41.

[15] Wahlstrom J, Gillberg C, Gustavson KH, Holmgren G. A Swedish multicenter study. Am J Med Genet 1986;23:403-8.

[16] Tranebjaerg L, Kure P. Prevalence of fra (X) and other specific diagnoses in autistic individuals in a Danish county. Am J Med Genet 1991;38:212-4.

[17] Ke Y, Zhang EE, Hagihara K, Wu D, Pang Y, Klein R, et al. Deletion of Shp2 in the brain leads to defective proliferation and differentiation in neural stem cells, and early postnatal lethality. Mol Cell Biol 2007;27:6706-17.

[18] Karbowniczek M, Cash T, Cheung M, Robertson GP, Astrinidis A, Henske EP. Regulation of B-Raf kinase activity by Tuberin and Rheb is mammalian target of Rapamycin (mTOR)-independent. J Biol Chem 2004;279:29930-7.

[19] Sarkozy A, Conti E, Digilio MC, Marino B, Morini E, Pacileo G, et al. J Med Genet 2004;41:e68.

[20] Tartaglia M, Mehler EL, Goldberg R, Zampino G, Brunner HG, Kremer H, et al. Mutations in PTPN11, encoding the protein tyrosine phosphatase SHP-2, cause Noonan syndrome. Nat Genet 2001;29:465-8.

[21] Schubbert S, Zenker M, Rowe SL, Boll S, Klein C, Bollag G, et al. Germline KRAS mutations cause Noonan syndrome. Nat Genet 2006;38:331-6.

[22] Herault J, Petit E, Martineau J, Perrot A, Lenoir P, Cherpi C, et al. Autism and genetics: clinical approach and association study with two markers of HRAS gene. Am J Med Genet 1995;60:276-81.

[23] Lee DA, Portnoy S, Hill P, Gillberg C, Patton MA. Psychological profile of children with Noonan syndrome. Dev Med Child Neurol 2005;47:35-8.

Journal of Human Genetics (2011) 56, 34–40

www.nature.com/jhg

ORIGINAL ARTICLE

A genome-wide association study identifies *RNF213* as the first Moyamoya disease gene

Fumiaki Kamada[1], Yoko Aoki[1], Ayumi Narisawa[1,2], Yu Abe[1], Shoko Komatsuzaki[1], Atsuo Kikuchi[3], Junko Kanno[1], Tetsuya Niihori[1], Masao Ono[4], Naoto Ishii[5], Yuji Owada[6], Miki Fujimura[2], Yoichi Mashimo[7], Yoichi Suzuki[7], Akira Hata[7], Shigeru Tsuchiya[3], Teiji Tominaga[2], Yoichi Matsubara[1] and Shigeo Kure[1,3]

Moyamoya disease (MMD) shows progressive cerebral angiopathy characterized by bilateral internal carotid artery stenosis and abnormal collateral vessels. Although ~15% of MMD cases are familial, the MMD gene(s) remain unknown. A genome-wide association study of 785 720 single-nucleotide polymorphisms (SNPs) was performed, comparing 72 Japanese MMD patients with 45 Japanese controls and resulting in a strong association of chromosome 17q25-ter with MMD risk. This result was further confirmed by a locus-specific association study using 335 SNPs in the 17q25-ter region. A single haplotype consisting of seven SNPs at the *RNF213* locus was tightly associated with MMD ($P=5.3\times10^{-10}$). *RNF213* encodes a really interesting new gene finger protein with an AAA ATPase domain and is abundantly expressed in spleen and leukocytes. An RNA *in situ* hybridization analysis of mouse tissues indicated that mature lymphocytes express higher levels of *Rnf213* mRNA than their immature counterparts. Mutational analysis of *RNF213* revealed a founder mutation, p.R4859K, in 95% of MMD families, 73% of non-familial MMD cases and 1.4% of controls; this mutation greatly increases the risk of MMD ($P=1.2\times10^{-43}$, odds ratio=190.8, 95% confidence interval=71.7–507.9). Three additional missense mutations were identified in the p.R4859K-negative patients. These results indicate that *RNF213* is the first identified susceptibility gene for MMD.
Journal of Human Genetics (2011) **56**, 34–40; doi:10.1038/jhg.2010.132; published online 4 November 2010

INTRODUCTION

'Moyamoya' is a Japanese expression for something hazy, such as a puff of cigarette smoke drifting in the air. In individuals with Moyamoya disease (MMD), there is a progressive stenosis of the internal carotid arteries; a fine network of collateral vessels, which resembles a puff of smoke on a cerebral angiogram, develops at the base of the brain (Figure 1a).[1,2] This steno-occlusive change can cause transient ischemic attacks and/or cerebral infarction, and rupture of the collateral vessels can cause intracranial hemorrhage. Children under 10 years of age account for nearly 50% of all MMD cases.[3]

The etiology of MMD remains unclear, although epidemiological studies suggest that bacterial or viral infection may be implicated in the development of the disease.[4] Growing attention has been paid to the upregulation of arteriogenesis and angiogenesis associated with MMD because chronic ischemia in other disease conditions is not always associated with a massive development of collateral vessels.[5,6] Several angiogenic growth factors are thought to have functions in the development of MMD.[7]

Several lines of evidence support the importance of genetic factors in susceptibility to MMD.[8] First, 10–15% of individuals with MMD have a family history of the disease.[9] Second, the concordance rate of MMD in monozygotic twins is as high as 80%.[10] Third, the prevalence of MMD is 10 times higher in East Asia, especially in Japan (6 per 100 000 population), than in Western countries.[3] Familial MMD may be inherited in an autosomal dominant fashion with low penetrance or in a polygenic manner.[11] Linkage studies of MMD families have revealed five candidate loci for an MMD gene: chromosomes 3p24–26,[12] 6q25,[13] 8q13–24,[10] 12p12–13[10] and 17q25.[14] However, no susceptibility gene for MMD has been identified to date.

We collected 20 familial cases of MMD to investigate linkage in the five putative MMD loci. However, a definitive result was not obtained for any of the loci. We then hypothesized that there might be a founder mutation among Japanese patients with MMD because the prevalence of MMD is unusually high in Japan.[15] Genome-wide and locus-specific association studies were performed and successfully identified a single gene, *RNF213*, linked to MMD. We report here a strong association between MMD onset and a founder mutation in *RNF213*, as well as the expression profiles of *RNF213*, in various tissues.

[1]Department of Medical Genetics, Tohoku University School of Medicine, Sendai, Japan; [2]Department of Neurosurgery, Tohoku University School of Medicine, Sendai, Japan; [3]Department of Pediatrics, Tohoku University School of Medicine, Sendai, Japan; [4]Department of Pathology, Tohoku University School of Medicine, Sendai, Japan; [5]Department of Microbiology and Immunology, Tohoku University School of Medicine, Sendai, Japan; [6]Department of Organ Anatomy, Yamaguchi University Graduate School of Medicine, Ube, Japan and [7]Department of Public Health, Graduate School of Medicine, Chiba University, Chiba, Japan
Correspondence: Dr S Kure, Department of Pediatrics, Tohoku University School of Medicine, 1-1 Seiryo-machi, Aoba-ku, Miyagi, Sendai 980-8574, Japan.
E-mail: kure@med.tohoku.ac.jp
Received 30 September 2010; accepted 1 October 2010; published online 4 November 2010

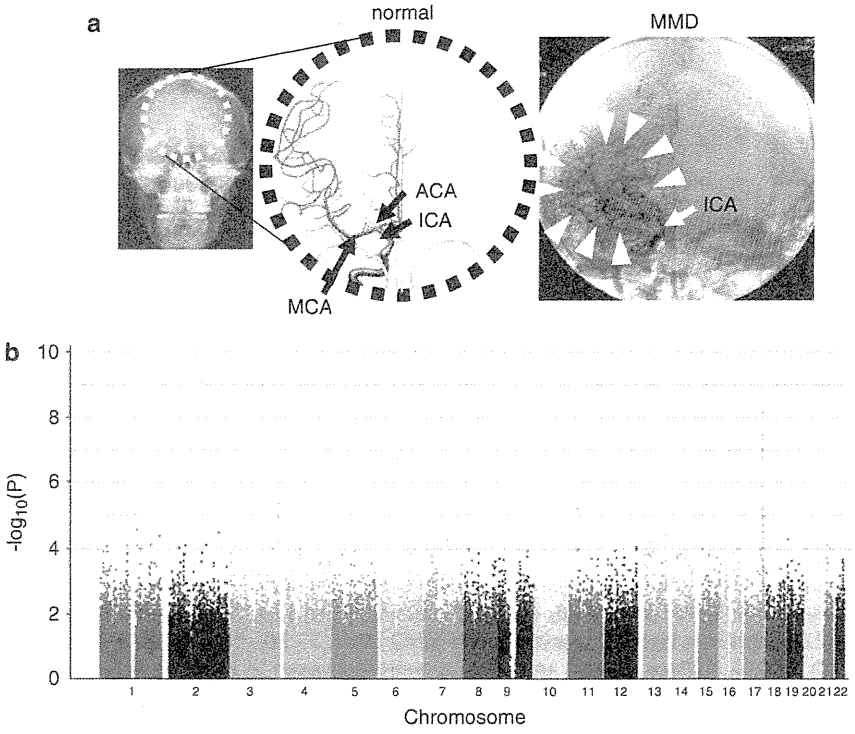

Figure 1 (**a**) Abnormal brain vessels in MMD. The dotted circle indicates the X-ray field of cerebral angiography (left panel). Normal structures of the right internal carotid artery (ICA), anterior cerebral artery (ACA) and middle cerebral artery (MCA) are illustrated (middle panel). The arrowheads indicate abnormal collateral vessels appearing like a puff of smoke in the angiogram of an individual with MMD (right panel). Note that ACA and MCA are barely visible, because of the occlusion of the terminal portion of the ICA. (**b**) Manhattan plot of the 785 720 SNPs used in the genome-wide association analysis of MMD patients. Note that the SNPs in the 17q25-ter region reach a significance of $P<10^{-8}$.

MATERIALS AND METHODS

Affected individuals

Genomic DNA was extracted from blood and/or saliva samples obtained from members of the families with MMD (Supplementary Figure 1), MMD patients with no family history and control subjects. All of the subjects were Japanese. MMD was diagnosed on the basis of guidelines established by the Research Committee on Spontaneous Occlusion of the Circle of Willis of the Ministry of Health and Welfare of Japan. This study was approved by the Ethics Committee of Tohoku University School of Medicine. Total RNA samples were purified from leukocytes using an RNeasy mini kit (Qiagen, Hilden, Germany) and used as templates for cDNA synthesis with an Oligo $(dT)_{20}$ primer and SuperScript II reverse transcriptase according to the manufacturer's instructions (Invitrogen, Carlsbad, CA, USA).

Linkage analysis

For the linkage analysis, DNA samples were genotyped for 36 microsatellite markers within five previously reported MMD loci using the ABI 373A DNA Sequencer (Applied Biosystems, Foster City, CA, USA). Pedigrees and haplotypes were constructed with the Cyrillic version 2.1 software (Oxfordshire, UK). Multipoint analyses were conducted using the GENEHUNTER 2 software (http://www.broadinstitute.org/ftp/distribution/software/genehunter/). Statistical analysis was performed with SPSS version 14.0J (SPSS, Tokyo, Japan).

Genome-wide and locus-specific association studies

A genome-wide association study was performed using a group of 72 MMD patients, which consisted of 64 patients without a family history of MMD and 8 probands of MMD families. The Illumina Human Omni-Quad 1 chip (Illumina, San Diego, CA, USA) was used for genotyping, and single-nucleotide polymorphisms (SNPs) with a genotyping completion rate of 100% were used for further statistical analysis (785 720 out of 1 140 419 SNPs). Genotyping data from 45 healthy Japanese controls were obtained from the database at the International HapMap Project web site. The 785 720 SNPs were statistically analyzed using the PLINK software (http://pngu.mgh.harvard.edu/~purcell/plink/index.shtml). For a locus-specific association study, we used 63 DNA samples consisting of 58 non-familial MMD patients and 5 probands of MMD families. A total of 384 SNPs within chromosome 17q25-ter were genotyped (Supplementary Table 1), using the GoldenGate Assay and a custom SNP chip (Illumina). Genotyping data for 45 healthy Japanese were used as a control. Case–control single-marker analysis, haplotype frequency estimation and significance testing of differences in haplotype frequency were performed using the Haploview version 3.32 program (http://www.broad.mit.edu/mpg/haploview/).

Mutation detection

Mutational analyses of *RNF213* and *FLJ35220* were performed by PCR amplification of each coding exon and putative promoter regions, followed by direct sequencing. Genomic sequence data for the two genes were obtained from the National Center for Biotechnology Information web site (http://www.ncbi.nlm.nih.gov/) for design of exon-specific PCR primers. *RNF213* cDNA fragments were amplified from leukocyte mRNA for sequencing analysis. Sequencing of the PCR products was performed with the ABI BigDye Terminator Cycle Sequencing Reaction Kit using the ABI 310 Genetic Analyzer. Identified base changes were screened in control subjects. Statistical difference of the carrier frequency of each base change was estimated by Fisher's exact test (the MMD group vs the control group).

Quantitative PCR

MTC Multiple Tissue cDNA Panels (Clontech Laboratory, Madison, WI, USA) were the source of cDNAs from human cell lines, adult and fetal tissues. Mononuclear cells and polymorphonuclear cells were isolated from the fresh peripheral blood of healthy human adults using Polymorphprep (Cosmo Bio,

Carlsbad, CA, USA). T and B cells were isolated from the fresh peripheral blood of healthy human adults using the autoMACS separator (Militeny Biotec, Bergisch Gladbach, Germany). Total RNA was isolated from these cells with the RNeasy Mini Kit (Qiagen) following the manufacturer's instructions. We reverse transcribed 100 ng samples of total RNA into cDNAs using the High Capacity cDNA Reverse Transcription Kit (Applied Biosystems). Quantitative PCRs were performed in a final volume of 20 μl using the FastStart TaqMan Probe Master (Rox) (Roche, Madison, WI, USA), 5 μl of cDNA, 10 μM of *RNF*- or *GAPDH*-specific primers and 10 μM of probes (Universal ProbeLibrary Probe #80 for *RNF213* and Roche Probe #60 for *GAPDH*). All reactions were performed in triplicate using the ABI 7500 Real-Time PCR system (Applied Biosystems). Cycling conditions were 2 min at 50°C and 10 min at 95°C, followed by 40 cycles of 15 s at 95°C and 60 s at 60°C. Real-time PCR data were analyzed by the SDS version 1.2.1 software (Applied Biosystems). We evaluated the relative level of *RNF213* mRNA by determining the C_T value, the PCR cycle at which the reporter fluorescence exceeded the signal baseline. *GAPDH* mRNA was used as an internal reference for normalization of the quantitative expression values.

Multiplex PCR

MTC Multiple Tissue cDNA Panels (Clontech) were the source of human cell lines and cDNAs from human adult and fetal tissues. Multiplex PCRs were performed in a final volume of 20 μl using the Multiplex PCR Master Mix (Qiagen), 2 μl of cDNA, a 2 μM concentration of *RNF213* and a 10 μM concentration of *GAPDH*-specific primers. The samples were separated on a 2% agarose gel stained with ethidium bromide. Cycling conditions were 15 min at 94°C, followed by 30 cycles of 30 s at 94 °C, 30 s at 57 °C and 30 s at 72 °C. For normalization of the expression levels, we used *GAPDH* as an internal reference for each sample.

In situ hybridization (ISH) analysis

Paraffin-embedded blocks and sections of mouse tissues for ISH were obtained from Genostaff (Tokyo, Japan). The mouse tissues were dissected, fixed with Tissue Fixative (Genostaff), embedded in paraffin by proprietary procedures (Genostaff) and sectioned at 6 μm. To generate anti-sense and sense RNA probes, a 521-bp DNA fragment corresponding to nucleotide positions 470–990 of mouse *Rnf213* (BC038025) was subcloned into the pGEM-T Easy vector (Promega, Madison, WI, USA). Hybridization was performed with digoxigenin-labeled RNA probes at concentrations of 300 ng ml^{-1} in Probe Diluent-1 (Genostaff) at 60 °C for 16 h. Coloring reactions were performed with NBT/BCIP solution (Sigma-Aldrich, St Louis, MO, USA). The sections were counterstained with Kernechtrot stain solution (Mutoh, Tokyo, Japan), dehydrated and mounted with Malinol (Mutoh). For observation of *Rnf213* expression in activated lymphocytes, 10-week-old Balb/c mice were intraperitoneally injected with 100 μg of keyhole limpet hemocyanin and incomplete adjuvant and sacrificed in 2 weeks. The spleen of the mice was removed for Hematoxylin–eosin staining and ISH analyses.

RESULTS

Using 20 Japanese MMD families, we reevaluated the linkage mapped previously to five putative MMD loci. No locus with significant linkage, Lod score >3.0 or NPL score >4.0 was confirmed (Supplementary Figure 2). We conducted a genome-wide association study of 72 Japanese MMD cases. Single-marker allelic tests comparing the 72 MMD cases and 45 controls were performed for 785 720 SNPs using χ^2 statistics. These tests identified a single locus with a strong association with MMD ($P<10^{-8}$) on chromosome 17q25-ter (Figure 1b), which is in line with the latest mapping data of a MMD locus.[16] The SNP markers with $P<10^{-6}$ are listed in Table 1. To confirm this observation, we performed a locus-specific association study. A total of 384 SNP markers (Supplementary Table 1) were selected within the chromosome 17q25-ter region and genotyped in a set of 63 MMD cases and 45 controls. The SNP markers demonstrating a high association with MMD ($P<10^{-6}$) were clustered in a 151-kb region from base position 75 851 399–76 003 020 (SNP No.116–136 in

Table 1 A genome-wide association study of Japanese MMD patients and controls

	SNP	*Chromosome*	*Base position*	*Gene*	*Risk allele/ non-risk allele*	*Risk allele frequency in MMD*	*Risk allele frequency in controls*	χ^2	*P-value*	*Odds ratio*	*95% confidence interval*	
											Lower	*Upper*
1	rs11870849	17	76 025 668	*RNF213*	T/C	0.4792	0.1111	33.55	6.95E-09	7.36	3.532	15.34
2	rs6565681	17	75 963 089	*RNF213*	A/G	0.7361	0.3667	31.35	2.16E-08	4.819	2.733	8.489
3	rs7216493	17	75 941 953	*RNF213*	G/A	0.75	0.3889	30.39	3.53E-08	4.715	2.673	8.313
4	rs7217421	17	75 850 055	*RNF213*	A/G	0.6667	0.3	29.86	4.64E-08	4.666	2.642	8.237
5	rs12449863	17	75 857 806	*RNF213*	C/T	0.6667	0.3	29.86	4.64E-08	4.666	2.642	8.237
6	rs4890009	17	75 926 103	*RNF213*	G/A	0.8819	0.5778	28.5	9.38E-08	5.459	2.831	10.527
7	SNP17-75933731	17	75 933 731	*RNF213*	G/A	0.8819	0.5778	28.5	9.38E-08	5.458	2.831	10.527
8	rs7219131	17	75 867 365	*RNF213*	T/C	0.6667	0.3111	28.11	1.15E-07	4.429	2.517	7.794
9	rs6565677	17	75 932 037	*RNF213*	T/C	0.7431	0.3977	27.43	1.63E-07	4.378	2.483	7.722
10	rs4889848	17	75 969 256	*RNF213*	C/T	0.75	0.4111	26.99	2.05E-07	4.297	2.444	7.889
11	rs7224239	17	75 969 771	*RNF213*	A/G	0.8681	0.5667	26.99	2.05E-07	5.03	2.659	9.529

Abbreviations: MMD, moyamoya disease; SNP, single-nucleotide polymorphism.A genome-wide association study testing 1 140 419 SNPs on the Human Omni-Quad 1chip (Illumina, San Diego, CA, USA) was performed in 72 Japanese MMD cases. Single-marker allelic tests between the cases and controls were performed using χ^2 statistics for all markers. This table lists the 11 SNP markers with a significance of $P<10^{-6}$.

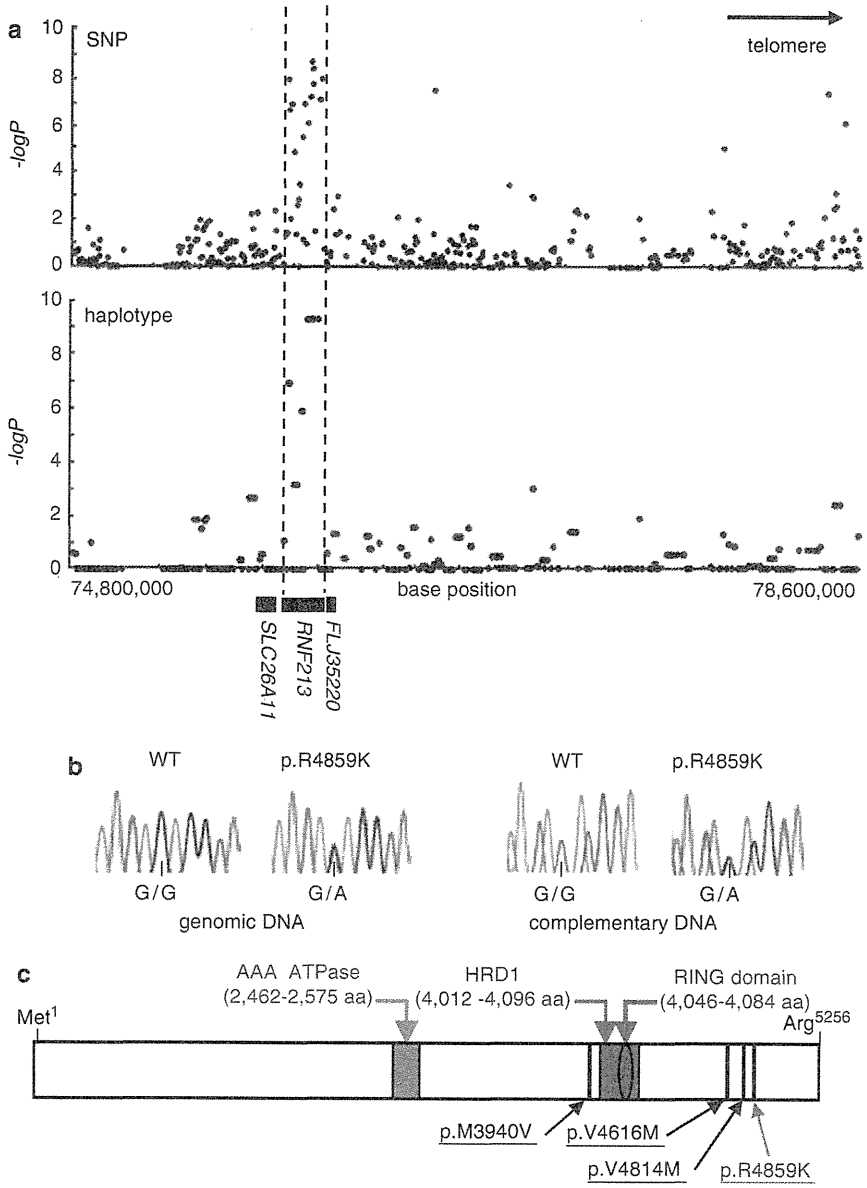

Figure 2 (**a**) Association analysis of 63 non-familial MMD cases and 45 control subjects. Statistical significance was evaluated by the χ^2-test. SNP markers with a strong association with MMD ($P<10^{-6}$) clustered in a 161-kb region (base position 75 851 399–76 012 838) indicated by two dotted lines (upper panel), which included the entire region of *RNF213* (lower panel). Haplotype analysis revealed a strong association ($P=5.3\times10^{-10}$) between MMD and a single haplotype located within *RNF213*. (**b**) Sequencing chromatograms of the identified MMD mutations. The left panel shows the sequences of an unaffected individual and a carrier of a p.R4859K heterozygous mutation. The right panel indicates the sequencing chromatograms of the leukocyte cDNA obtained from an unaffected individual and an individual with MMD who carries the p.R4859K mutation. Note that both wild-type and mutant alleles were expressed in leukocytes. (**c**) The structure of the RNF213 protein. The RNF213 protein contains three characteristic structures, the AAA-superfamily ATPase motif, the RING motif and the HMG-CoA reductase degradation motif. The positions of four mutations identified in MMD patients are underlined, including one prevalent mutation (red) and three private mutations (black).

Supplementary Table 1); this entire region was within the *RNF213* locus (Figure 2a). A single haplotype determined by seven SNPs (SNP Nos.130–136 in Supplementary Table 1) that resided in the 3′ region of *RNF213* was strongly associated with MMD onset ($P=5.3\times10^{-10}$). Analysis of the linkage disequilibrium block indicated that this haplotype was not in complete linkage disequilibrium with any other haplotype in this region (Supplementary Figure 3). These results strongly suggest that a founder mutation may exist in the 3′ part of *RNF213*.

Mutational analysis of the entire coding and promoter regions of *RNF213* and *FLJ35220*, a gene 3′ adjacent to *RNF213*, revealed that 19 of the 20 MMD families shared the same single base substitution, c.14576G>A, in exon 60 of *RNF213* (Figure 2b and Table 2). This nucleotide change causes an amino-acid substitution from arginine^{4859} to lysine^{4859} (p.R4859K). The p.R4859K mutation was identified in 46 of 63 non-familial MMD cases (73%), including 45 heterozygotes and a single homozygote (Table 3). Both the wild-type and the p.R4859K mutant alleles were co-expressed in leukocytes

Table 2 Nucleotide changes with amino-acid substitutions identified in the sequencing analysis of *RNF213* and *FLJ35220*

Gene	Exon	Nucleotide change[a] (amino-acid substitution)	Genotype (allele)		P-value[b]	χ^2 (df=1)[c]	Odds ratio (95% CI)
			Non-familial cases	Control subjects			
RNF213	29	c.7809C>A (p.D2603E)	2/63 (2/126)	15/381 (15/762)	0.77	0.09	0.80 (0.2–3.6)
RNF213	41	c.11818A>G (p.M3940V)	1/63 (1/126)	0/388 (0/776)	0.01	6.17	ND
RNF213	41	c.11891A>G (p.E3964G)	4/63 (4/126)	3/55 (4/110)	0.84	0.04	1.2 (0.3–5.5)
RNF213	52	c.13342G>A (p.A4448T)	4/63 (4/126)	2/53 (2/106)	0.53	0.39	1.7 (0.3–9.8)
RNF213	56	c.13846G>A (p.V4616M)	1/63 (1/126)	0/388 (0/776)	0.01	6.17	ND
RNF213	59	c.14440G>A (p.V4814M)	1/63 (1/126)	0/388 (0/776)	0.01	6.17	ND
RNF213	60	c.14576G>A (p.R4859K)	46/63 (47/126)	6/429 (6/858)	1.2×10^{-43}	298.1	190.8 (71.7–507.9)
FLJ35220		None					

Abbreviations: ND, not determined; SNP, single-nucleotide polymorphism.
[a]Nucleotide numbers of *RNF213* cDNA are counted from the A of the ATG initiator methionine codon (NCBI Reference sequence, NP_065965.4).
[b]*P*-values were calculated by Fisher's exact test.
[c]Genotypic distribution (carrier of the polymorphism vs non-carrier).

Table 3 Association of the p.R4859K (c.14576G>A) mutation with MMD

	Total	Genotype		
		wt/wt (%)	*wt/p.R4859K* (%)	*p.R4859K/ p.R4859K* (%)[d]
Members of 19 MMD families[a]				
Affected	42	0	39 (92.9)	3 (7.1)
Not affected	28	15 (53.6)	13 (46.4)	0
Individuals without a family history of MMD[b,c]				
Affected	63	17 (27.0)	45 (71.4)	1 (1.6)
Not affected	429	423 (98.6)	6 (1.4)	0

Abbreviations: MMD, moyamoya disease.
[a]Entire distribution, $\chi^2=29.4$, $P=4.2\times10^{-7}$.
[b]Entire distribution, $\chi^2=298.2$, $P=1.8\times10^{-65}$.
[c]Genotypic distribution (p.R4859K carrier vs non-carrier), $\chi^2=298.1$, $P=1.2\times10^{-43}$, odds ratio=190.8 (95% CI=71.7–507.9).
[d]The age of onset and initial symptoms of the four homozygotes were comparable to those of the 84 heterozygous patients.

in three patients heterozygous for the p.R4859K mutation (Figure 2b), excluding the possible instability of the mutant *RNF213* mRNA. Additional missense mutations, p.M3940V, p.V4616M and p.V4814M, were detected in three non-familial MMD cases without the p.R4859K mutation (Figure 2c). These mutations were not found in 388 control subjects and were detected in only one patient, suggesting that they were private mutations (Table 2). No copy number variation or mutation was identified in the *RNF213* locus of 12 MMD patients using comparative genome hybridization microarray analysis (Supplementary Figure 4). In total, 6 of the 429 control subjects (1.4%) were found to be heterozygous carriers of p.R4859K. Therefore, we concluded that the p.R4859K mutation increases the risk of MMD by a remarkably high amount (odds ratio=190.8 (95% confidence interval=71.7–507.9), $P=1.2\times10^{-43}$) (Table 3). It was recently reported that an SNP (ss161110142) in the promoter region of *RPTOR*, which is located ~150 kb downstream from *RNF213*, was associated with MMD.[17] Genotyping of the SNP in *RPTOR* showed that the *RNF213* p.R4859K mutation was more strongly associated with MMD than ss161110142 (Supplementary Figure 1).

RNF213 encodes a protein with 5256 amino acids harboring a RING (really interesting new gene) finger motif, suggesting that it functions as an E3 ubiquitin ligase (Figure 2c). It also has an AAA ATPase domain, which is characteristic of energy-dependent unfoldases.[18] To our knowledge, RNF213 is the first RING finger protein known to contain an AAA ATPase domain. The expression profile of *RNF213* has not been previously fully characterized. We performed a quantitative reverse transcription PCR analysis in various human tissues and cells. *RNF213* mRNA was highly expressed in immune tissues, such as spleen and leukocytes (Figure 3a and Supplementary Figure 5). Expression of *RNF213* was detected in fractions of both polymorphonuclear cells and mononuclear cells and was found in both B and T cell fractions (Supplementary Figure 6). A low but significant expression of *RNF213* was also observed in human umbilical vein endothelial cells and human pulmonary artery smooth muscle cells. Cellular expression was not enhanced in tumor cell lines, compared with leukocytes. In human fetal tissues, the highest expression was observed in leukocytes and the thymus (Supplementary Figure 6E). The expression of *RNF213* was surprisingly low in both adult and fetal brains. Overall, *RNF213* was ubiquitously expressed, and the highest expression was observed in immune tissues.

We studied the cellular expression of *Rnf213* in mice. The ISH analysis of spleen showed that *Rnf213* mRNA was present in small mononuclear cells, which were mainly localized in the white pulps (Figures 3b–g). The ISH signals were also detected in the primary follicles in the lymph node and in thymocytes in the medulla of the thymus (Supplementary Figure 7). To study *Rnf213* expression in activated lymphocytes we immunized mice with keyhole limpet hemocyanin, and examined *Rnf213* mRNA in spleen by ISH analysis. Primary immunization with keyhole limpet hemocyanin antigen revealed that the expression of *Rnf213* in the secondary follicle is as high as in the primary follicle in the lymph node (Supplementary Figure 8). In an E16.5 mouse embryo, expression was observed in the medulla of the thymus and in the cells around the mucous palatine glands (Supplementary Figure 9). These findings suggest that mature lymphocytes in a static state express *Rnf213* mRNA at a higher level than do their immature counterparts.

DISCUSSION

We identified a susceptibility locus for MMD by genome-wide and locus-specific association studies. Further sequencing analysis revealed a founder missense mutation in *RNF213*, p.R4859K, which was tightly associated with MMD onset. Identification of a founder mutation in individuals with MMD would resolve the following recurrent

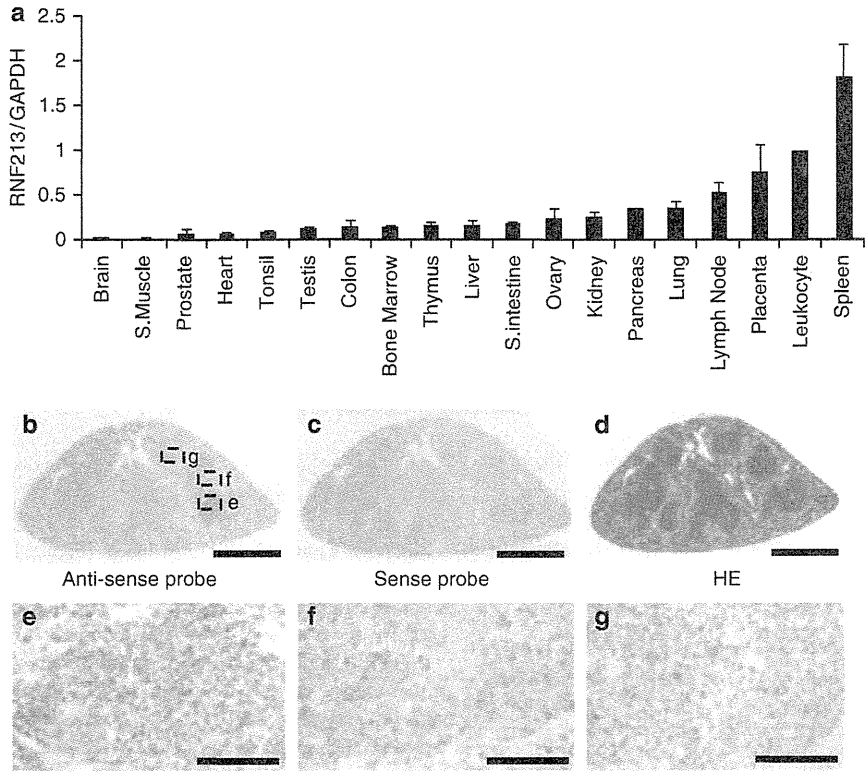

Figure 3 Expression of human RNF213 and murine Rnf213. (**a**) RT-PCR analysis of RNF213 mRNA in various human tissues. The expression levels of *RNF213* mRNA in various adult human tissues were evaluated by quantitative PCR using *GAPDH* mRNA as a control. The signal ratio of *RNF213* mRNA to *GAPDH* mRNA in each sample is shown on the vertical axis. (**b–g**) *In situ* hybridization (ISH) analysis of Rnf213 mRNA in mouse spleen. Specific signals for *Rnf213* mRNA were detected by ISH analysis with the anti-sense probe (**b**) but not with the sense probe (**c**). Hematoxylin–eosin staining of the mouse spleen (**d**). Signals for the *Rnf213* mRNA were observed in small mononuclear cells, which were mainly localized in the white pulps (dotted square, **e**) and partially distributed in the red pulps (dotted squares, **f** and **g**). Panels e, f and g show the high-magnification images of the corresponding fields in panel b. Scale bars, 1 mm (**b–d**) and 50 μm (**e–g**).

questions:[2,19] (i) why is MMD more prevalent in East Asia than in Western countries? The carrier frequency of p.R4859K in Japan is 1/72 (Table 2). In contrast, we found no p.R4859K carrier in 400 Caucasian controls (data not shown). Furthermore, no mutation was identified in five Caucasian patients with MMD after the full sequencing of *RNF213*. These results suggest that the genetic background of MMD in Asian populations is distinct from that in Western populations and that the low incidence of MMD in Western countries may be attributable to a lack of the founder *RNF213* mutation. (ii) Is unilateral involvement a subtype of MMD or a different disease?[2] We collected DNA samples from six patients with unilateral involvement and found a p.R4859K mutation in four of them (data not shown), suggesting that bilateral and unilateral MMD share a genetic background. (iii) Is pre-symptomatic diagnosis of MMD possible? In the present study, MMD never developed in the 15 mutation-negative family members in the 19 MMD families with the p.R4859K mutation (Table 3 and Supplementary Figure 1), suggesting the feasibility of presymptomatic diagnosis or exclusion by genetic testing.

How the mutant RNF213 protein causes MMD remains to be elucidated. The expression of *RNF213* was more abundant in a subset of leukocytes than in the brain, suggesting that blood cells have a function in the etiology of MMD. This observation agrees with a previous report that MMD patients have systemic angiopathy.[20] Recent studies have suggested that the postnatal vasculature can form through vasculogenesis, a process by which endothelial progenitor cell are recruited from the splenic pool and differentiate into mature endothelial cells.[21] Levels of endothelial progenitor cells in the peripheral blood are increased in MMD patients.[22] *RNF213* may be expressed in splenic endothelial progenitor cells and mutant *RNF213* might dysregulate the function of the endothelial progenitor cells. Further research is necessary to elucidate the role of *RNF213* in the etiology of MMD.

CONFLICT OF INTEREST

The authors declare no conflict of interest.

ACKNOWLEDGEMENTS

We thank all of the patients and their families for participating in this study. We also thank Dr Hidetoshi Ikeda at the Department of Neurosurgery, Tohoku University School of Medicine and Drs Toshiaki Hayashi and Reizo Shirane at the Department of Neurosurgery, Miyagi Children's Hospital, Sendai, Japan for patient recruitment. We are grateful to Ms Kumi Kato for technical assistance. This study was supported by grants from the Ministry of Education, Culture, Sports, Science and Technology, Japan and by the Research Committee on Moyamoya Disease of the Ministry of Health, Labor and Welfare, Japan.

1 Suzuki, J. & Takaku, A. Cerebrovascular 'moyamoya' disease. Disease showing abnormal net-like vessels in base of brain. *Arch. Neurol.* **20,** 288–299 (1969).
2 Suzuki, J. *Moyamoya Disease* (Springer-Verlag: Berlin, 1983).
3 Oki, K., Hoshino, H. & Suzuki, N. In: *Moyamoya Disease Update*, (eds Cho B.K., Tominaga T.) 29–34 (Springer: New York, 2010).
4 Phi, J. H., Kim, S. K., Wang, K. C. & Cho, B. K. In: *Moyamoya Disease Update*, (eds Cho B.K., Tominaga T). 82–86, (Springer: New York, 2010).
5 Yoshihara, T., Taguchi, A., Matsuyama, T., Shimizu, Y., Kikuchi-Taura, A., Soma, T. *et al.* Increase in circulating CD34-positive cells in patients with angiographic evidence of moyamoya-like vessels. *J. Cereb. Blood Flow Metab.* **28,** 1086–1089 (2008).
6 Achrol, A. S., Guzman, R., Lee, M. & Steinberg, G. K. Pathophysiology and genetic factors in moyamoya disease. *Neurosurg. Focus.* **26,** E4 (2009).
7 Scott, R. M. & Smith, E. R. Moyamoya disease and moyamoya syndrome.. *N. Engl. J. Med.* **360,** 1226–1237 (2009).
8 Kure, S. In: *Moyamoya Disease Update* (eds Cho B.K., Tominaga T.) 41–45 (Springer: Tokyo, 2010).
9 Kuriyama, S., Kusaka, Y., Fujimura, M., Wakai, K., Tamakoshi, A., Hashimoto, S. *et al.* Prevalence and clinicoepidemiological features of moyamoya disease in Japan: findings from a nationwide epidemiological survey. *Stroke.* **39,** 42–47 (2008).
10 Sakurai, K., Horiuchi, Y., Ikeda, H., Ikezaki, K., Yoshimoto, T., Fukui, M. *et al.* A novel susceptibility locus for moyamoya disease on chromosome 8q23. *J. Hum. Genet.* **49,** 278–281 (2004).
11 Nanba, R., Kuroda, S., Tada, M., Ishikawa, T., Houkin, K. & Iwasaki, Y. Clinical features of familial moyamoya disease. *Childs. Nerv. Syst.* **22,** 258–262 (2006).
12 Ikeda, H., Sasaki, T., Yoshimoto, T., Fukui, M. & Arinami, T. Mapping of a familial moyamoya disease gene to chromosome 3p24.2-p26. *Am. J. Hum. Genet.* **64,** 533–537 (1999).
13 Inoue, T. K., Ikezaki, K., Sasazuki, T., Matsushima, T. & Fukui, M. Linkage analysis of moyamoya disease on chromosome 6. *J. Child. Neurol.* **15,** 179–182 (2000).
14 Yamauchi, T., Tada, M., Houkin, K., Tanaka, T., Nakamura, Y., Kuroda, S. *et al.* Linkage of familial moyamoya disease (spontaneous occlusion of the circle of Willis) to chromosome 17q25.. *Stroke.* **31,** 930–935 (2000).
15 Wakai, K., Tamakoshi, A., Ikezaki, K., Fukui, M., Kawamura, T., Aoki, R. *et al.* Epidemiological features of moyamoya disease in Japan: findings from a nationwide survey. *Clin. Neurol. Neurosurg.* **99**(Suppl 2), S1–S5 (1997).
16 Mineharu, Y., Liu, W., Inoue, K., Matsuura, N., Inoue, S., Takenaka, K. *et al.* Autosomal dominant moyamoya disease maps to chromosome 17q25.3. *Neurology.* **70,** 2357–2363 (2008).
17 Liu, W., Hashikata, H., Inoue, K., Matsuura, N., Mineharu, Y., Kobayashi, H. *et al.* A rare Asian founder polymorphism of Raptor may explain the high prevalence of Moyamoya disease among East Asians and its low prevalence among Caucasians. *Environ. Health. Prev. Med.* **15,** 94–104 (2010).
18 Lupas, A. N. & Martin, J. AAA proteins.. *Curr. Opin. Struct. Biol.* **12,** 746–753 (2002).
19 Ikezaki, K. In: *Moyamoya disease* (eds Ikezaki K., Loftus C. M.) 43–75 (Thieme: New York, 2001).
20 Ikeda, E. Systemic vascular changes in spontaneous occlusion of the circle of Willis. *Stroke.* **22,** 1358–1362 (1991).
21 Zampetaki, A., Kirton, J. P. & Xu, Q. Vascular repair by endothelial progenitor cells. *Cardiovasc. Res.* **78,** 413–421 (2008).
22 Rafat, N., Beck, G., Pena-Tapia, P. G., Schmiedek, P. & Vajkoczy, P. Increased levels of circulating endothelial progenitor cells in patients with Moyamoya disease. *Stroke.* **40,** 432–438 (2009).

Supplementary Information accompanies the paper on Journal of Human Genetics website (http://www.nature.com/jhg)

Journal of Human Genetics (2011) 56, 91–93

www.nature.com/jhg

SHORT COMMUNICATION

Androgenetic/biparental mosaicism in a girl with Beckwith–Wiedemann syndrome-like and upd(14)pat-like phenotypes

Kazuki Yamazawa[1,5], Kazuhiko Nakabayashi[2], Kentaro Matsuoka[3], Keiko Masubara[1], Kenichiro Hata[2], Reiko Horikawa[4] and Tsutomu Ogata[1]

This report describes androgenetic/biparental mosaicism in a 4-year-old Japanese girl with Beckwith–Wiedemann syndrome (BWS)-like and paternal uniparental disomy 14 (upd(14)pat)-like phenotypes. We performed methylation analysis for 18 differentially methylated regions on various chromosomes, genome-wide microsatellite analysis for a total of 90 loci and expression analysis of *SNRPN* in leukocytes. Consequently, she was found to have an androgenetic 46,XX cell lineage and a normal 46,XX cell lineage, with the frequency of the androgenetic cells being roughly calculated as 91% in leukocytes, 70% in tongue tissues and 79% in tonsil tissues. It is likely that, after a normal fertilization between an ovum and a sperm, the paternally derived pronucleus alone, but not the maternally derived pronucleus, underwent a mitotic division, resulting both in the generation of the androgenetic cell lineage by endoreplication of one blastomere containing a paternally derived pronucleus and in the formation of the normal cell lineage by union of paternally and maternally derived pronuclei. It appears that the extent of overall (epi)genetic aberrations exceeded the threshold level for the development of BWS-like and upd(14)pat-like phenotypes, but not for the occurrence of other imprinting disorders or recessive Mendelian disorders.
Journal of Human Genetics (2011) **56**, 91–93; doi:10.1038/jhg.2010.142; published online 11 November 2010

Keywords: androgenesis; Beckwith–Wiedemann syndrome; mosaicism; upd(14)pat

INTRODUCTION

A pure androgenetic human with paternal uniparental disomy for all chromosomes is incompatible with life because of genomic imprinting.[1,2] However, a human with an androgenetic cell lineage could be viable in the presence of a normal cell lineage. Indeed, an androgenetic cell lineage has been identified in six liveborn individuals with variable phenotypes.[3–7] All the androgenetic cell lineages have a 46,XX karyotype, and this is consistent with the lethality of an androgenetic 46,YY cell lineage.

Here, we report on a girl with androgenetic/biparental mosaicism, and discuss the underlying factors for the phenotypic development.

CASE REPORT

This patient was conceived naturally to non-consanguineous and healthy parents. At 24 weeks gestation, the mother was referred to us because of threatened premature delivery. Ultrasound studies showed Beckwith–Wiedemann syndrome (BWS)-like features,[8] such as macroglossia, organomegaly and umbilical hernia, together with polyhydramnios and placentomegaly. The mother repeatedly received amnioreduction and tocolysis.

She was delivered by an emergency cesarean section because of preterm rupture of membranes at 34 weeks of gestation. Her birth weight was 3730 g (+4.8 s.d. for gestational age), and her length 45.6 cm (+0.7 s.d.). The placenta weighed 1040 g (+7.3 s.d.).[9] She was admitted to a neonatal intensive care unit due to asphyxia. Physical examination confirmed a BWS-like phenotype. Notably, chest roentgenograms delineated mild bell-shaped thorax characteristic of paternal uniparental disomy 14 (upd(14)pat),[10] although coat hanger appearance of the ribs indicative of upd(14)pat was absent (Supplementary Figure 1). She was placed on mechanical ventilation for 2 months, and received tracheostomy, glossectomy and tonsillectomy in her infancy, due to upper airway obstruction. She also had several clinical features occasionally reported in BWS[8] (Supplementary Table 1). Her karyotype was 46,XX in all the 50 lymphocytes analyzed. On the last examination at 4 years of age, she showed postnatal growth failure and severe developmental retardation.

[1]Department of Molecular Endocrinology, National Research Institute for Child Health and Development, Tokyo, Japan; [2]Department of Maternal-Fetal Biology, National Research Institute for Child Health and Development, Tokyo, Japan; [3]Division of Pathology, National Medical Center for Children and Mothers, Tokyo, Japan and [4]Division of Endocrinology and Metabolism, National Medical Center for Children and Mothers, Tokyo, Japan
[5]Current address: Department of Physiology, Development & Neuroscience, University of Cambridge, Cambridge, UK.
Correspondence: Dr T Ogata, Department of Molecular Endocrinology, National Research Institute for Child Health and Development, 2-10-1 Ohkura, Setagaya, Tokyo 157-8535, Japan.
E-mail: tomogata@nch.go.jp
Received 9 September 2010; revised 18 October 2010; accepted 22 October 2010; published online 11 November 2010

MOLECULAR STUDIES

This study was approved by the Institutional Review Board Committee at the National Center for Child health and Development, and performed after obtaining informed consent.

Methylation analysis

We first performed bisulfite sequencing for the *H19*-DMR (differentially methylated region) and KvDMR1 as a screening of BWS[11,12] and that for the IG-DMR and the *MEG3*-DMR as a screening of upd(14)pat,[10] using leukocyte genomic DNA. Paternally derived clones were predominantly identified for the four DMRs examined (Figure 1a). We next performed combined bisulfite restriction analysis for multiple DMRs, as reported previously.[13] All the autosomal DMRs exhibited markedly skewed methylation patterns consistent with predominance of paternally inherited clones, whereas the *XIST*-DMR on the X chromosome showed a normal methylation pattern (Figure 1a).

Genome-wide microsatellite analysis

Microsatellite analysis was performed for 90 loci with high heterozygosities in the Japanese population.[14] Major peaks consistent with paternal uniparental isodisomy and minor peaks of maternal origin were identified for at least one locus on each chromosome, with the minor peaks of maternal origin being more obvious in tongue and tonsil tissues than in leukocytes (Figure 1b and Supplementary Table 2). There were no loci with three or four peaks indicative of chimerism. The frequency of the androgenetic cells was calculated as 91% in leukocytes, 70% in tongue cells and 79% in tonsil cells, although the estimation apparently was a rough one (for details, see Supplementary Methods).

Expression analysis

We examined *SNRPN* expression, because *SNRPN* showed strong expression in leukocytes (for details, see Supplementary Data). *SNRPN* expression was almost doubled in the leukocytes of this patient (Figure 1c).

DISCUSSION

These results suggest that this patient had an androgenetic 46,XX cell lineage and a normal 46,XX cell lineage. In this regard, both the androgenetic and the biparental cell lineages appear to have derived from a single sperm and a single ovum, because a single haploid genome of paternal origin and that of maternal origin were identified in this patient by genome-wide microsatellite analysis. Thus, it is likely that after a normal fertilization between an ovum and a sperm, the paternally derived pronucleus alone, but not the maternally derived pronucleus, underwent a mitotic division, resulting both in the generation of the androgenetic cell lineage by endoreplication of

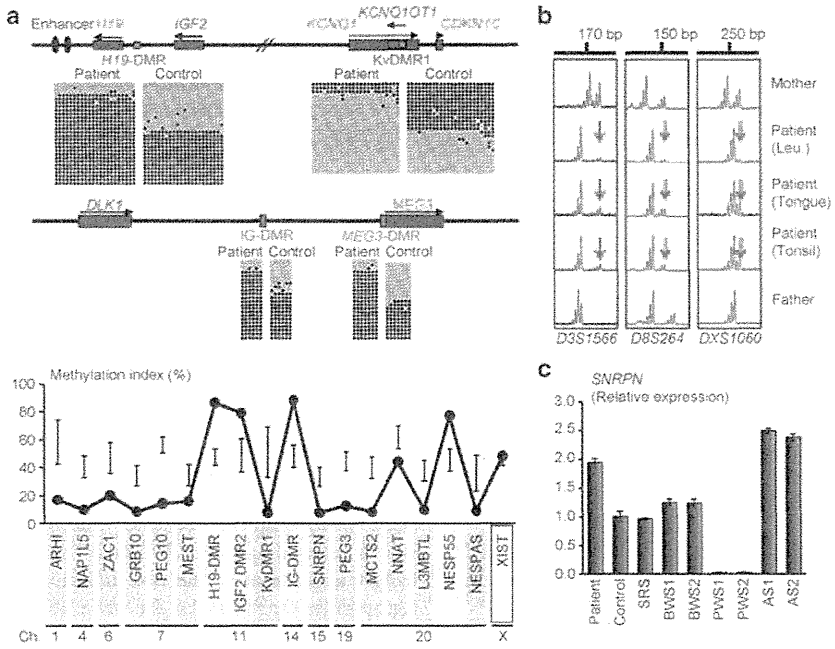

Figure 1 Representative molecular results. (**a**) Methylation analysis. Upper part: Bisulfite sequencing data for the *H19*-DMR and the KvDMR1 on 11p15.5, and those for the IG-DMR and the *MEG3*-DMR on 14q32.2. Each line indicates a single clone, and each circle denotes a CpG dinucleotide; filled and open circles represent methylated and unmethylated cytosines, respectively. Paternally expressed genes are shown in blue, maternally expressed gene in red, and the DMRs in green. The *H19*-DMR, the IG-DMR, and the *MEG3*-DMR are usually methylated after paternal transmission and unmethylated after maternal transmission, whereas the KvDMR1 is usually unmethylated after paternal transmission and methylated after maternal transmission.[10,11] Lower part: Methylation indices (the ratios of methylated clones) obtained from the COBRA analyses for the 18 DMRs. The DMRs highlighted in blue and pink are methylated after paternal and maternal transmissions, respectively. The black vertical bars indicate the reference data (maximum – minimum) in leukocyte genomic DNA of 20 normal control subjects (the *XIST*-DMR data are obtained from 16 control females). (**b**) Representative microsatellite analysis. Major peaks of paternal origin and minor peaks of maternal origin (red arrows) have been identified in this patient. The minor peaks of maternal origin are more obvious in tongue and tonsil tissues than in leukocytes (Leu.). (**c**) Relative expression level (mean ± s.d.) of *SNRPN*. The data are normalized against *TBP*. SRS: an SRS patient with an epimutation (hypomethylation) of the *H19*-DMR; BWS1: a BWS patient with an epimutation (hypermethylation) of the *H19*-DMR; BWS2: a BWS patient with upd(11)pat; PWS1: a Prader-Willi syndrome (PWS) patient with upd(15)mat; PWS2: a PWS patient with an epimutation (hypermethylation) of the *SNRPN*-DMR; AS1: an Angelman syndrome (AS) patient with upd(15)pat; and AS2: an AS patient with an epimutation (hypomethylation) of the *SNRPN*-DMR. The data were obtained using an ABI Prism 7000 Sequence Detection System (Applied Biosystems).

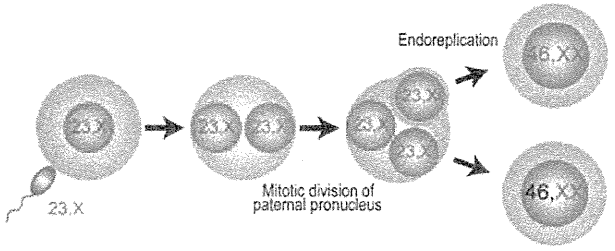

Figure 2 Schematic representation of the generation of the androgenetic/biparental mosaicism. Polar bodies are not shown.

one blastomere containing a paternally derived pronucleus and in the formation of the normal cell lineage by union of paternally and maternally derived pronuclei (Figure 2). This model has been proposed for androgenetic/biparental mosaicism generated after fertilization between a single ovum and a single sperm.[5,15,16] The normal methylation pattern of the *XIST*-DMR is explained by assuming that the two X chromosomes in the androgenetic cell lineage undergo random X-inactivation, as in the normal cell lineage. Furthermore, the results of microsatellite analysis imply that the androgenetic cells were more prevalent in leukocytes than in tongue and tonsil tissues.

A somatic androgenetic cell lineage has been identified in seven liveborn patients including this patient (Supplementary Table 1).[3–7] In this context, leukocytes are preferentially utilized for genetic analyses in human patients, and detailed examinations such as analyses of plural DMRs are necessary to detect an androgenetic cell lineage. Thus, the hitherto identified patients would be limited to those who had androgenetic cells as a predominant cell lineage in leukocytes probably because of a stochastic event and received detailed molecular studies. If so, an androgenetic cell lineage may not be so rare, and could be revealed by detailed analyses as well as examinations of additional tissues in patients with relatively complex phenotypes, as observed in the present patient.

Phenotypic features in androgenetic/biparental mosaicism would be determined by several factors. They include (1) the ratio of two cell lineages in various tissues/organs, (2) the number of imprinted domains relevant to specific features (for example, dysregulation of the imprinted domains on 11p15.5 and 14q32.2 is involved in placentomegaly[9,17]), (3) the degree of clinical effects of dysregulated imprinted domains (an (epi)dominant effect has been assumed for the 11p15.5 imprinted domains[18]), (4) expression levels of imprinted genes in androgenetic cells (although *SNRPN* expression of this patient was consistent with androgenetic cells being predominant in leukocytes, complicated expression patterns have been identified for several imprinted genes in both androgenetic and parthenogenetic fetal mice, probably because of perturbed *cis*- and *trans*-acting regulatory mechanisms[19]) and (5) unmasking of possible paternally inherited recessive mutation(s) in androgenetic cells. Thus, in this patient, it appears that the extent of overall (epi)genetic aberrations exceeded the threshold level for the development of BWS-like and upd(14)pat-like body and placental phenotypes, but remained below the threshold level for the occurrence of other imprinting disorders or recessive Mendelian disorders.

CONFLICT OF INTEREST

The authors declare no conflict of interest.

ACKNOWLEDGEMENTS

This work was supported by grants from the Ministry of Health, Labor, and Welfare, and the Ministry of Education, Science, Sports and Culture.

1 Surani, M. A., Barton, S. C. & Norris, M. L. Development of reconstituted mouse eggs suggests imprinting of the genome during gametogenesis. *Nature* **308,** 548–550 (1984).
2 McGrath, J. & Solter, D. Completion of mouse embryogenesis requires both the maternal and paternal genomes. *Cell* **37,** 179–183 (1984).
3 Hoban, P. R., Heighway, J., White, G. R., Baker, B., Gardner, J., Birch, J. M. *et al.* Genome-wide loss of maternal alleles in a nephrogenic rest and Wilms' tumour from a BWS patient. *Hum. Genet.* **95,** 651–656 (1995).
4 Bryke, C. R., Garber, A. T. & Israel, J. Evolution of a complex phenotype in a unique patient with a paternal uniparental disomy for every chromosome cell line and a normal biparental inheritance cell line. *Am. J. Hum. Genet.* **75**(Suppl), 831 (2004).
5 Giurgea, I., Sanlaville, D., Fournet, J. C., Sempoux, C., Bellanne-Chantelot, C. & Touati, G. Congenital hyperinsulinism and mosaic abnormalities of the ploidy. *J. Med. Genet.* **43,** 248–254 (2006).
6 Wilson, M., Peters, G., Bennetts, B., McGillivray, G., Wu, Z. H., Poon, C. *et al.* The clinical phenotype of mosaicism for genome-wide paternal uniparental disomy: two new reports. *Am. J. Med. Genet. Part A* **146A,** 137–148 (2008).
7 Reed, R. C., Beischel, L., Schoof, J., Johnson, J., Raff, M. L. & Kapur, R. P. Androgenetic/biparental mosaicism in an infant with hepatic mesenchymal hamartoma and placental mesenchymal dysplasia. *Pediatr. Dev. Pathol.* **11,** 377–383 (2008).
8 Jones, K. L. *Smith's Recognizable Patterns of Human Malformation* 6th edn. (Elsevier Saunders: Philadelphia, 2006).
9 Kagami, M., Yamazawa, K., Matsubara, K., Matsuo, N. & Ogata, T. Placentomegaly in paternal uniparental disomy for human chromosome 14. *Placenta* **29,** 760–761 (2008).
10 Kagami, M., Sekita, Y., Nishimura, G., Irie, M., Kato, F., Okada, M. *et al.* Deletions and epimutations affecting the human 14q32.2 imprinted region in individuals with paternal and maternal upd(14)-like phenotypes. *Nat. Genet.* **40,** 237–242 (2008).
11 Yamazawa, K., Kagami, M., Nagai, T., Kondoh, T., Onigata, K., Maeyama, K. *et al.* Molecular and clinical findings and their correlations in Silver-Russell syndrome: implications for a positive role of IGF2 in growth determination and differential imprinting regulation of the IGF2-H19 domain in bodies and placentas. *J. Mol. Med.* **86,** 1171–1181 (2008).
12 Weksberg, R., Shuman, C. & Beckwith, J. B. Beckwith-Wiedemann syndrome. *Eur. J. Hum. Genet.* **18,** 8–14 (2010).
13 Yamazawa, K., Nakabayashi, K., Kagami, M., Sato, T., Saitoh, S., Horikawa, R. *et al.* Parthenogenetic chimaerism/mosaicism with a Silver-Russell syndrome-like phenotype. *J. Med. Genet.* **47,** 782–785 (2010).
14 Ikari, K., Onda, H., Furushima, K., Maeda, S., Harata, S. & Takeda, J. Establishment of an optimized set of 406 microsatellite markers covering the whole genome for the Japanese population. *J. Hum. Genet.* **46,** 207–210 (2001).
15 Kaiser-Rogers, K. A., McFadden, D. E., Livasy, C. A., Dansereau, J., Jiang, R., Knops, J. F. *et al.* Androgenetic/biparental mosaicism causes placental mesenchymal dysplasia. *J. Med. Genet.* **43,** 187–192 (2006).
16 Kotzot, D. Complex and segmental uniparental disomy updated. *J. Med. Genet.* **45,** 545–556 (2008).
17 Monk, D., Arnaud, P., Apostolidou, S., Hills, F. A., Kelsey, G., Stanier, P. *et al.* Limited evolutionary conservation of imprinting in the human placenta. *Proc. Natl. Acad. Sci. USA.* **103,** 6623–6628 (2006).
18 Azzi, S., Rossignol, S., Steunou, V., Sas, T., Thibaud, N., Danton, F. *et al.* Multilocus methylation analysis in a large cohort of 11p15-related foetal growth disorders (Russell Silver and Beckwith Wiedemann syndromes) reveals simultaneous loss of methylation at paternal and maternal imprinted loci. *Hum. Mol. Genet.* **18,** 4724–4733 (2009).
19 Ogawa, H., Wu, Q., Komiyama, J., Obata, Y. & Kono, T. Disruption of parental-specific expression of imprinted genes in uniparental fetuses. *FEBS Lett.* **580,** 5377–5384 (2006).

Supplementary Information accompanies the paper on Journal of Human Genetics website (http://www.nature.com/jhg)

Endocrine Journal 2011, **58** (2), 117-121

ORIGINAL

GATA3 abnormalities in six patients with HDR syndrome

Maki Fukami[1], Koji Muroya[2], Tetsuo Miyake [1),3)], Manami Iso[1], Fumiko Kato[1], Hisashi Yokoi[4], Yoshimi Suzuki[5], Koji Tsubouchi[6], Yoshiko Nakagomi[7], Nobuyuki Kikuchi[8], Reiko Horikawa[9] and Tsutomu Ogata[1]

[1] *Department of Molecular Endocrinology, National Research Institute for Child Health and Development, Tokyo 157-8535, Japan*
[2] *Department of Endocrinology and Metabolism, Kanagawa Children's Medical Center, Yokohama 232-8555, Japan*
[3] *Department of Pediatrics, St. Marianna University Hospital, Kawasaki 216-8511, Japan*
[4] *Department of Internal Medicine, Japanese Red Cross Nagoya First Hospital, Nagoya 453-8511, Japan*
[5] *Department of Pediatrics, Atsumi Hospital, Tawara 441-3415, Japan*
[6] *Department of Pediatrics, Mino Municipal Hospital, Mino 501-3746, Japan*
[7] *Department of Pediatrics, Yamanashi University Hospital, Yamanashi 400-8510, Japan*
[8] *Department of Pediatrics, Yokohama City University Hospital, Yokohama 232-0024, Japan*
[9] *Division of Endocrinology and Metabolism, National Medical Center for Children and Mothers, Tokyo 157-8535, Japan*

Abstract. *GATA3* mutations cause HDR (*h*ypoparathyroidism, sensorineural *d*eafness, and *r*enal dysplasia) syndrome and, consistent with the presence of the second DiGeorge syndrome locus (*DGS2*) proximal to *GATA3*, distal 10p deletions often leads to HDR and DiGeorge syndromes. Here, we report on six Japanese patients with *GATA3* abnormalities. Cases 1–5 had a normal karyotype, and case 6 had a 46,XX,del(10)(p15) karyotype. Cases 1–6 had two or three of the HDR triad features. Case 6 had no DiGeorge syndrome phenotype except for hypoparathyroidism common to HDR and DiGeorge syndromes. Mutation analysis showed heterozygous *GATA3* mutations in cases 1–5, i.e., c.404–405insC (p.P135fsX303) in case 1, c.700T>C & c.708–709insC (p.F234L & p.S237fsX303) on the same allele in case 2, c.737-738insG (p.G246fsX303) in case 3, c.824G>T (p.W275L) in case 4, and IVS5+1G>C (splice error) in case 5. Deletion analysis of chromosome 10p revealed loss of *GATA3* and preservation of *D10S547* in case 6. The results are consistent with the previous finding that *GATA3* mutations are usually identified in patients with two or three of the HDR triad features, and provide supportive data for the mapping of *DGS2* in the region proximal to *D10S547*.

Key words: HDR syndrome, *GATA3*, DiGeorge syndrome, *DGS2*, Phenotypic spectrum

HDR (*h*ypoparathyroidism, sensorineural *d*eafness, and *r*enal dysplasia) syndrome is an autosomal dominant disorder first reported by Bilous *et al.* [1]. This condition is primarily caused by haploinsufficiency of *GATA3* on chromosome 10p15, although *GATA3* mutations have not been identified in a small portion of patients with clinical features compatible with HDR syndrome [2, 3]. *GATA3* consists of six exons, and encodes a transcription factor with two transactivating domains and two zinc finger domains on exons 2–6 [2]. *GATA3* is expressed in the developing parathyroid glands, inner ears, and kidneys, together with thymus and central nervous system (CNS) [4, 5].

Distal 10p deletions involving *GATA3* often lead to DiGeorge syndrome associated with hypoplastic thymus, T-cell immunodeficiency, hypoparathyroidism, congenital cardiac defects, and facial dysmorphism, in addition to HDR syndrome [6, 7]. Thus, deletion mappings have been performed, localizing the second DiGeorge syndrome locus (*DGS2*) to a ~1 cM region proximal to *D10S547* (the locus order: 10pter–*GATA3*–*D10S547*–*DGS2*–10cen) [6, 7].

Here, we report clinical and molecular findings in five patients with intragenic *GATA3* mutations and one patient with distal 10p deletion involving *GATA3*, and discuss the clinical features in *GATA3* mutation posi-

Received Aug. 4, 2010; Accepted Dec. 16, 2010 as K10E-234
Released online in J-STAGE as advance publication Jan. 13, 2011

Correspondence to: Tsutomu Ogata, Department of Molecular Endocrinology, National Research Institute for Child Health and Development, 2-10-1 Okura Setagaya-ku, Tokyo 157-8535, Japan.
E-mail: tomogata@nch.go.jp

Table 1 Summary of six patients with *GATA3* mutation or deletion

	Case 1	Case 2	Case 3	Case 4	Case 5	Case 6
Present age	40 years	39 years	4 years	31 years	17 years	4 years
Sex	Female	Female	Male	Female	Male	Female
Karyotype	46,XX	46,XX	46,XY	46,XX	46,XY	46,XX,del(10)(p15)
Hypoparathyroidism	Yes	Yes	Yes	Yes	Yes	Yes
Symptom	Convulsion	Tetany	No[b]	Convulsion	Convulsion	Convulsion
Ca (mg/dL)	3.4	3.4	2.7	4.3	3.0	4.7
P (mg/dL)	8.0	7.9	8.1	7.9	8.7	8.6
Intact PTH (pg/mL)	Undetected	Undetected	14	Undetected	Undetected	15
Age at diagnosis	10 years	13 years	17 months	3 years	17 months	2 weeks
Sensorineural deafness	Yes	Yes	No	Yes	Yes	Yes
Hearing level (dB)[a]	50 (B)	>70 (B)	Normal	60 (B)	50 (B)	90 (B)
Age at diagnosis	13 years	6 years		11 years	12 months	6 months
Renal lesion	Yes	Yes	Yes	Equivocal[c]	Yes	Yes
Malformation	RH (L)	PCD (B)	PD (R)	Absent	RH (L)	VUR (B)
Age at diagnosis	9 years	27 years	17 months		17 months	2 months

Abbreviations: PTH, parathyroid hormone; dB, decibel; B, bilateral; L, left; R, right; RH, renal hypoplasia; PCD, pelvicalyceal deformity; PD, pelvic duplication; and VUR, vesicoureteral reflux.
[a] Degree of hearing loss: normal, <25 dB; mild 26–40 dB; moderate 41–55 dB; moderately severe, 56–70 dB; and profound, >90 dB.
[b] Hypocalcemia was revealed by routine biochemical studies, when this boy was admitted because of bronchopneumonia.
[c] Renal malformation was absent, but renal dysfunction with increased serum creatinine was noticed during pregnancy.
Normal reference data: Ca: 8.84–10.44 mg/dL; P: 4.5–6.5 mg/dL; and intact PTH: 10–65 pg/mL.

tive patients and the chromosomal location of *DGS2*.

Patients and Methods

Patients

We studied six hitherto unreported Japanese patients (cases 1–6) with two or three HDR triad features. Cases 1–5 had a normal karyotype, and case 6 had a 46,XX,del(10)(p15) karyotype. Cases 1–4 and 6 were apparently sporadic cases, whereas case 5 was a possible familial case: the father received renal dialysis due to chronic renal failure from his twenties, and the paternal grandmother had unilateral renal hypoplasia, although they lacked clinical features suggestive of hypoparathyroidism and hearing difficulty.

Clinical phenotypes of the HDR triad features are summarized in Table 1. Hypoparathyroidism was noticed by convulsion in cases 1 and 4–6 and by tetany in case 2; in case 3, it was incidentally found by biochemical examinations at the time of admission due to bronchopneumonia. After confirming parathyroid hormone deficiency, 1α(OH) vitamin D therapy was started, successfully normalizing serum calcium and phosphate values in cases 1–6. Sensorineural deafness was demonstrated in cases 1, 2, and 4–6 by auditory brainstem response or audiometry, and they required hearing aids in their daily life. Case 3 had no hearing difficulty with normal auditory brainstem response. Renal lesion was radiologically confirmed in cases 1–3, 5, and 6. Although case 4 had no discernible renal malformation, she manifested renal dysfunction during pregnancy. In addition, case 6 exhibited developmental delay but lacked hypoplastic thymus, T-cell immunodeficiency, congenital cardiac defects, and facial dysmorphism characteristic of DiGeorge syndrome.

Mutation analysis of GATA3

This study was approved by the Institutional Review Board Committee at National Center for Child Health and Development. After obtaining informed consent, leukocyte genomic DNA samples of cases 1–6 were amplified by PCR for the coding regions on exons 2–6 and their flanking splice sites, and the PCR products were subjected to direct sequencing from both directions on a CEQ 8000 autosequencer (Beckman Coulter, Fullerton, CA). The primer sequences and the PCR conditions were as described previously [2, 3]. To confirm a heterozygous mutation, the corresponding PCR products were subcloned with a TOPO TA Cloning Kit (Life Technologies, Carlsbad, CA), and normal and mutant alleles were sequenced separately.